F. ÖZTÜRK

OPTIMAL EXCLUSION ZONE ESTIMATION FOR CO-EXISTENCE OF GEOSTATIONARY AND NON-GEOSTATIONARY SATELLITE NETWORKS

THE GRADUATE SCHOOL OF NATURAL AND APPLIED SCIENCES
OF
ATILIM UNIVERSITY

FAİK ÖZTÜRK

DOCTOR OF PHILOSOPHY THESIS
IN
THE DEPARTMENT OF ELECTRICAL AND ELECTRONICS ENGINEERING

JUNE 2022

ATILIM UNIVERSITY 2022

OPTIMAL EXCLUSION ZONE ESTIMATION FOR CO-EXISTENCE OF GEOSTATIONARY AND NON-GEOSTATIONARY SATELLITE NETWORKS

A THESIS SUBMITTED TO
THE GRADUATE SCHOOL OF NATURAL AND APPLIED SCIENCES
OF
ATILIM UNIVERSITY

BY

FAİK ÖZTÜRK

IN PARTIAL FULFILLMENT OF THE REQUIREMENTS
FOR
THE DEGREE OF DOCTOR OF PHILOSOPHY
IN
THE DEPARTMENT OF ELECTRICAL AND ELECTRONICS ENGINEERING

JUNE 2022

Approval of the Graduate School of Natural and Applied Sciences, Atilim University.

_____

Prof. Dr. Ender Keskinkılıç
Director

I certify that this thesis satisfies all the requirements as a thesis for the degree of **Doctor of Philosophy in Department of Electrical and Electronics Engineering Atılım University**.

_____

Assoc. Prof. Dr. Kemal Efe Eseller
Head of Department

This is to certify that we have read the thesis OPTIMAL EXCLUSION ZONE ESTIMATION FOR CO-EXISTENCE OF GEOSTATIONARY AND NON-GEOSTATIONARY SATELLITE NETWORKS submitted by FAİK ÖZTÜRK and that in our opinion it is fully adequate, in scope and quality, as a thesis for the degree of Doctor of Philosophy.

_____	_____
Prof. Dr. Ali Kara Co-Supervisor	Prof. Dr. Elif Aydın Supervisor

Examining Committee Members:

Prof. Dr. Tolga Girici
Electrical-Electronics Eng. Dept., TOBB ETU _____

Prof. Dr. Elif Aydın
Electrical-Electronics Eng. Dept., Atılım University _____

Prof. Dr. Reşat Özgür Doruk
Electrical-Electronics Eng. Dept., Atılım University _____

Assoc. Prof. Dr. Mehmet Ünlü
Electrical-Electronics Eng. Dept. TOBB ETU _____

Asst. Prof. Dr. Yaser Dalveren
Electrical-Electronics Eng. Dept., Atılım University _____

Date: 08.06.2022

I hereby declare that all information in this document has been obtained and presented in accordance with academic rules and ethical conduct. I also declare that, as required by these rules and conduct, I have fully cited and referenced all material and results that are not original to this work.

Name, Last Name : Faik Öztürk

Signature :

ABSTRACT

OPTIMAL EXCLUSION ZONE ESTIMATION FOR CO-EXISTENCE OF GEOSTATIONARY AND NON-GEOSTATIONARY SATELLITE NETWORKS

Öztürk, Faik
PhD., Department of Electrical and Electronics Engineering
Supervisor : Prof. Dr. Elif Aydın
Co-Supervisor : Prof. Dr. Ali Kara

June 2022, 72 pages

In this thesis, the co-existence downlink interference from a typical Low Earth Orbit (LEO) constellation to earth stations of Geostationary Earth Orbit (GEO) satellites is analysed by performing minimization of Exclusion Zone (EZ) on the equatorial region. Using the Genetic Algorithm (GA), a multi-objective optimization problem (MOP) is formulated for non-dominant solutions set based on Exclusive Angle (EA) minimization and bandwidth utilization of the LEO communication link. At transmission bit rates of 100 Mbps and 200 Mbps, it is shown that the EA can be reduced up to % 21.3 and % 19.6, respectively, when compared to the initial anchor point. For the LEO communication system, the proposed optimal operational setting minimizes interference risk to the GEO satellite system as well as ensuring Quality of Service (QoS). Additionally, analysis and comparative evaluation of interference mitigation methods for coexisting Non-Geostationary Earth (NGEO) and Geostationary Earth (GEO) systems are discussed. Afterwards, the quantitative performance assessment of Spatial Isolation (SI), Power Control (PC), and Spatial Isolation-Based Link Adaptation (SILA) methodologies is performed. When compared to SI and PC techniques, the SILA technique utilizes the EA methodology more effectively. In various operating settings, the EA can be reduced up to % 8 for

100 Mbps and % 8.5 for 200 Mbps transmission bit rates when the PC method and the SILA method are combined. The performance assessment presented in this study may assist the satellite operator or decision-maker in determining the suitable mitigation strategy to apply in the event of co-existence interference.

Keywords: satellite communication, co-existence interference, exclusion zone, spatial isolation-based link adaptation, multi-objective optimization.

ÖZ

YERDURAĞAN YÖRÜNGELİ VE YERDURAĞAN YÖRÜNGELİ OLMAYAN UYDU AĞLARININ BİRLİKTE VARLIĞI İÇİN UYGUN DIŞLAMA BÖLGESİ TAHMİNİ

Öztürk, Faik
Doktora, Elektrik-Elektronik Mühendisliği Bölümü
Tez Yöneticisi : Prof. Dr. Elif Aydın
Ortak Tez Yöneticisi : Prof. Dr. Ali Kara

Haziran 2022, 72 sayfa

Bu tezde, ekvator bölgesinde tipik bir Alçak Yörünge takımuydusu (AYT)'ndan Yerdurağan Yörünge (YDY) uydularının yer istasyonlarına yönelik, uyduların bir arada çalışması sebebiyle ortaya çıkabilecek enterferans, dışlama bölgesi daraltılarak analiz edilmektedir. Bu amaçla, Genetik Algoritma (GA) kullanılarak, AYT haberleşme linkinin dışlama açı minimizasyonu ve bant genişliği kullanımına dayalı baskın olmayan çözüm seti elde edilmesi için çok amaçlı bir optimizasyon problemi (ÇOP) tanımlanmıştır. 100 Mbps ve 200 Mbps veri hızlarında, başlangıç noktasına kıyasla dışlama açısının sırasıyla % 21.3 ve % 19.6'ya kadar azaltılabileceği gösterilmiştir. AYT iletişim sistemi için önerilen optimum operasyonel link parametre ayarlaması için sonuçlar incelendiğinde, YDY uydu sistemine yönelik enterferans riski en aza indirilmekte ve yeterli servis kalitesi temin edilmektedir. Bu çalışmada ayrıca bir arada var olan Yerdurağan Olmayan Yörünge (YDOY) ve YDY sistemleri için enterferans azaltma yöntemlerinin analizi ve karşılaştırmalı değerlendirmesi tartışılmaktadır. Bunun için, Uzaysal Izolasyon (UI), Güç Kontrolü (GK) ve Uzaysal Izolasyon Tabanlı Link Uyarlaması (UITLU) metodolojilerinin niceliksel performans değerlendirmesi yapılmıştır. UI ve GK teknikleri ile karşılaştırıldığında, UITLU

tekniğinin dışlama açısı metodolojisini daha etkin bir şekilde kullandığı gösterilmektedir. Çeşitli operasyonel koşullarda, GK yöntemi ve UITLU yöntemi birlikte uygulandığında ise, Dışlama Açısı (DA), 100 Mbps veri hızı için % 8'e, 200 Mbps veri hızı için % 8.5'e kadar düşürülebilmektedir. Bu çalışmada sunulan performans değerlendirmesi, uydu operatörüne veya karar vericiye, farklı yörünge uydularının bir arada operasyonu sebebiyle ortaya çıkabilecek enterferansın önlenmesi için uygulanacak enterferans önleme stratejisini belirlemede yardımcı olmaktadır.

Anahtar Kelimeler: Uydu haberleşmesi, bir arada bulunma enterferansı, dışlama bölgesi, uzaysal izolasyon tabanlı link uyarlaması, çok amaçlı optimizasyon.

To my family

ACKNOWLEDGMENTS

I would like to express my special appreciation and thanks to my advisors, Prof. Dr. Elif Aydın and Prof. Dr. Ali Kara, for their encouragement, invaluable guidance, helpful support throughout my research study inspired me to work hard, confident, and continual.

I shall also thank to my thesis committee members, Prof. Dr. Tolga Girici and Assoc. Prof. Dr. Mehmet Ünlü for offering constructive criticism, insightful recommendations, and patience that cannot be underestimated. I would also thank to my examining committee members, Prof. Dr. Reşat Özgür Doruk and Asst. Prof. Dr. Yaser Dalveren, for their invaluable comments.

Furthermore, I thank the members of satellite frequency monitoring department of TÜRKSAT A.Ş.

Finally, no word can express my thanks to my wife, who has made sacrifices on my behalf. I am really deeply indebted to her for her supporting.

TABLE OF CONTENTS

APPENDICES

LIST OF TABLES

TABLES

LIST OF FIGURES

FIGURES

LIST OF SYMBOLS/ABBREVIATIONS

ACM	Adaptive Coding and Modulation
DL	Deep Learning
DSSS	Direct-Sequence Spread Spectrum
DVB-S2	Second Generation Standard for Satellite Broad-Band Services
DVB-S2X	Extension of Second-Generation Standard for Satellite Broad-Band Services
EA	Exclusive Angle
EIRP	Effective Isotropic Radiated Power
EIRPD	Effective Isotropic Radiated Power Flux Density
EPFD	Equivalent Power Flux Density
EZ	Exclusion Zone
FEC	Forward Error Correction
GA	Genetic Algorithm
GEO	Geostationary Earth Orbit
IoT	Internet of Things
ITU	International Telecommunication Union
LEO	Low Earth Orbit
LSTM	Long Short-term Memory
MEO	Medium Earth Orbit
ML	Machine Learning
MLSN	Multi-layer Satellite Networks
MODCOD	Modulation and Coding
MOP	Multi-objective Optimization Problem
MOGA	Multi-objective Genetic Algorithm
NGEO	Non-Geostationary Earth Orbit
NOMA	Non-orthogonal Multiple Access
PC	Power Control
PFD	Power Flux Density

PSK	Phase-Shift Keying
QoS	Quality of Service
SF	Spreading Factor
SI	Spatial Isolation
SILA	Spatial Isolation-based Link Adaptation
SOP	Single-Objective Optimization Problem
SS	Spread Spectrum

CHAPTER 1

INTRODUCTION

According to the distance between the satellite and the surface of Earth, satellite orbits are defined respectively Geostationary Earth Orbit (GEO), Medium Earth Orbit (MEO) and Low Earth Orbit (LEO). LEO satellite networks propose the minimum latency, link degradation, and manufacturing and launch costs compared to MEO and GEO satellite networks. As the demands for low cost broadband communication increasing year by year, it is aimed to provide high-quality access around the world using LEO satellites. This has resulted in the LEO networks acquiring more importance in the satellite industry. In the next several years, it is projected that tens of thousands of LEO satellites will be in orbit [1,2]. On the other hand, the interference coordination is a problem when the co-existence of GSO and NGSO satellites. The presence of GEO satellites for years and their active utilization plans for the foreseeable future, along with the ambitious business plans of LEO satellite operators, make interference minimization a complex situation to solve.

The in-line interference situation is the most critical interference case, in particular between GEO and Non-Geostationary Earth Orbit (NGEO) satellite systems [3-6]. Higher latitude GEO earth stations are less likely to face in-line interference with a LEO satellite network than lower latitude GEO earth stations. On the other hand, GEO earth stations positioned near the equator, may be subject to in-line interference with LEO satellites due to their proximity to the equator [7]. According to operational evaluation above this issue, the downlink interference from the LEO satellite to the GEO earth station is the most problematic interference case [8,9]. It's possible that a GEO earth station in-line with a LEO satellite will be affected by interference in this situation. Moreover, if LEO satellites are using the same spectrum allocation as the GEO network, GEO terminals that are placed inside the service area of LEO satellites may face downlink interference from LEO satellites. Consequently, while planning

LEO and GEO satellite missions, it is critical to guarantee that both orbits are coordinated as much as possible with one another.

Large number of researches have been conducted to eliminate the effect of interference between the two satellite networks. Power Control (PC), antenna selection, geographic separation between earth stations, satellite diversification, earth station diversity, link controlling, and coordination mechanisms are all mentioned in [10] as methods for the mitigating interference. It is recommended that spatial separation be used in LEO-GEO coexistence to keep interference levels at manageable ranges [11]. Additionally, by analyzing operational settings, an interference mitigation strategy that takes spatial isolation and link balancing into account concurrently is proposed in [12]. In [13], a technique for acquiring accurate progressive pitch parameters for the LEO system is provided that is based on interference mitigation for the GEO satellite network. The interference between NGEO and geosynchronous satellites is investigated using this probabilistic estimate of the position of a LEO satellite [14]. Additional cognitive radio approaches have been suggested, including static and coordinated/uncoordinated interference aligning, and also cognitive range-based power control strategies [15,16]. Beam power control algorithm is proposed to optimize the throughput of LEO satellites depend on the quality of service (QoS) requirements of the GEO satellites [17]. In [18,19], beam hopping strategies based on interference assessment are developed for successfully managing the communication traffic. An enhanced adaptive modulation and coding (AMC) system for spectral co-operation of GEO and NGEO systems is recommended [20]. By targeting on ground stations with low latitude, phased array antennas are suggested for proper tilting of LEO satellites [21]. In [22], a number of PC strategies are applied to minimize in-line interference induced by NGEO satellites. To minimize interference between NGEO and GEO networks, solutions including spot turn-off and frequency division algorithms have been presented [23]. A cooperative beam association and power management methodology for the LEO system to cooperate bandwidth assignment with GEO system, as well as a dynamic resource distribution based on beam hopping, are presented [24,25]. A few dynamic spectrum-sharing and cooperative service strategies, taking into account power allocation, are provided in [26-28] in order to minimize co-existence interference. Various spectrum sensing methodologies are proposed for the analysis of

the spectrum management among GEO and LEO systems [29–31]. An efficient way for the interference mitigation among GEO and LEO satellite systems is presented in [32,33] using Non-Orthogonal Multiple Access (NOMA) techniques. Using an integrated wireless multimedia sensor and taking into account dynamic frequency assignment, a spectrum-sharing strategy for the cognitive radio is provided in [34]. Moreover, a Deep Learning (DL)-based prediction model with artificial neural networks and bidirectional long short-term memory (LSTM) is recommended for generating the spectral scenario [35].

The communication link standard is critical in mitigating interference between different satellite systems in orbit. A new digital video broadcasting standard for satellites (DVB-S2X) was defined based on existing DVB-S2 standard. It incorporates sharper roll-offs and improved modulation and coding (MODCOD), as well as a more advanced superframing structure [36]. As shown in [37], the DVB-S2X standard can also be used for both fixed and mobile communication services. In addition, it is possible to provide more optionality in the DVB-S2X standard by including adaptive coding and modulation (ACM) [38]. On the other hand, DVB-S2X uses a low SNR (signal-to-noise ratio) model to minimize the impact of interference. Spread Spectrum (SS) is a methodology used in DVB systems that preserves the link's QoS while eliminating interference [39]. SS techniques are already being employed well in anti-jamming operations [40]. Various implementations of Direct-Sequence Spread Spectrum (DSSS) are discussed in [41,42]. [43] examines the anti-jamming effectiveness of multi-carrier DSSS systems and concludes that multi-carrier systems achieve comparable results to single-carrier systems. The DSSS technology for mobile broadband satellite network is being examined and evaluated, and it is being recommended as a suitable solution in [44]. Additionally, the role of multiple-access interference on the capacity of a LEO system is discussed [45].

Wide range of engineering issues have been solved using multi-objective optimization [46]. Multi-objective Optimization Problem (MOP) solutions are presented for vehicle engine bracket model [46], compact UV disinfection solutions [47], and multi-beam satellite power management [48]. Moreover, many other interference coordination approaches were developed based on it. The employment of Genetic Algorithms (GA) [46] is an appropriate mechanism of handling MOPs. The principle of survival of the

fittest provides a framework for GA's operation. Non-dominant solutions are selected to keep in the population while the population changes in GA. Numerous studies have shown that GA is capable of solving a wide variety of engineering challenges when structured as a MOP [49-53].

Improvements in interference mitigation strategies are witnessed throughout time as satellite technology advances. It is critical to study the benefits and improvements of various strategies and their commitment to interference minimization for co-existing NGEO and GEO systems in this respect. In interference mitigation studies, although different techniques such as planned orbit maneuvers on the equator are recommended for LEO systems, the performance of GEO systems may be affected due to the non-dynamic nature of these methods. Moreover, the QoS of the LEO system may not be guaranteed while trying to mitigate co-existence interference with these static methods. Therefore, more dynamic interference mitigation technologies are needed for co-existence of LEO and GEO systems. Especially, instead of optimizing the LEO communication link on the equatorial region, the efficiency of LEO communication decreases by preferring only planned orbit maneuvers and turning off LEO communication on the equator region to mitigate co-existence interference. Here, another interference mitigation approach, which is Exclusion Zone (EZ) geometry, that is representing the operational discrimination to mitigate interference from LEO system to GEO system evaluating both LEO and GEO satellites and ground stations locations, is not used efficiently. On the other hand, since these two-interference mitigation methods are not evaluated together, it is currently obtained limited performance for the co-existence LEO and GEO system. In addition, the fact that EZ geometry and LEO link optimization are not evaluated together in the operations on the equator region does not give the optimum network planning requirements to the LEO satellite operator that it needs operationally. At this stage, it is critical to implement flexibility into existing mitigation strategies by taking into consideration the practical key parameters as well as possible. The employment of the spatial isolation model in combination with the link adaption approach is a case of this flexibility in practice.

In this work, the downlink co-existence interference analyses from LEO system to GEO system are discussed. Using a typical LEO system and a reference GEO system,

a cognitive satellite system strategy is developed to increase GEO-LEO co-operability in the equatorial area. In order to accomplish this, an EZ in which the LEO satellites are turned off is designed, and an interference model is developed. This study aims to find out how to reduce the EZ under various operating situations. In the interference assessment, realistic satellite operating characteristics are taken into consideration. Radiation pattern calculations methodoligies for antennas [54,55] which are published by regulatory authorities are implemented in a straightforward way. In the same way, ITU Equivalent Power Flux Density (EPFD) limitations [56] are utilized in interference analysis to make a realistic evaluation of the situation. Following that, the GA is used to define and solve a MOP problem. The thesis-based MOP formulation represents a realistic operating situation based on system goals and limitations. MODCOD with spread spectrum (SS) and MODCOD without spread spectrum (SS) are both regarded as operational scenarios for the LEO communication link. A pareto front is obtained once the optimization problem is solved, showing both dominant and non-dominant solutions. Our findings indicate that the Exclusive Angle (EA) can be reduced by % 21.3 percent for a 100 Mbps transmission rate and it can be also reduced by % 19.6 for a 200 Mbps transmission rate in comparison to the initial anchor points. Rather of concentrating just on power, this research employs link adaptation based on power spectral density optimization considering bandwidth allocation, and MODCOD selection in combination with spatial isolation technique. This has led to the development of a dynamic interference mitigation method known as Spatial Isolation-Based Link Adaptation (SILA) [12].

In addition, the strengths and specific features of interference mitigation approaches are thoroughly examined, and a performance assessment is carried out to compare them. Prior to conducting quantitative assessments, it is necessary to identify interference mitigation approaches that may fulfill certain comparison assessment criteria. In this study, Spatial Isolation (SI) [3,8,11] and PC [7,16,19,22] are each evaluated against the SILA method [12] individually in a quantitative-based methodology. In contrast to other methodologies, these three are considered comparable owing to their concentration on communication link settings and spatial limitations. The interference model in [12] is used for performance evaluation and comparison of LEO-GEO interference mitigation strategies in this work. For the

comparative assessment of SI and SILA technique, comparison of EA allocation is performed for different MODCOD usage cases. Using the SILA approach, the EA can be reduced by 77.6% for the same MODCOD selection and it can be reduced by up to 82.1% for the MODCOD optimization. With the same MODCOD selection, the EA may be reduced by up to 77.6% for 200 Mbps data rate, and by up to 81.4% with MODCOD optimization.

PC, which is frequently utilized in interference mitigation studies, and SILA are compared in the other study. A single-objective optimization problem (SOP) based on the PC approach is defined and the communication bandwidth, power, and EA parameters are optimized appropriately. In the next step, these results are compared to those produced using SILA [12]. When results are analyzed attentively, the SILA offers more efficient bandwidth assignment than the PC method. Additionally, it presents a narrower EZ with a reduced EA. This helps operators improve bandwidth distribution and reduce LEO satellite turn-off time. Furthermore, when compared to the SOP formulation with the PC, the suggested MOP formulation with the SILA provides a possible number of options. Moreover, a novel MOP formulation is used to evaluate the efficiency of a joint implementation of the two interference mitigation strategies. The optimization problem solution indicates that the EA can be further minimize to 8% and 8.5% for 100 Mbps and 200 Mbps transmission rates, respectively. Finally, qualitative classifications of interference mitigation techniques are performed and their advantages and contributions are examined. Qualitative comparisons of existing interference mitigation approaches may assist users choose the best suitable one based on operating conditions, priorities, and hardware restrictions. As a result of this thesis' quantitative and qualitative assessment, new operational models may be developed for co-existing NGEO-GEO satellite systems.

To the authors' knowledge, this is the first study to present optimum solutions, comparative evaluation, and performance analysis of various interference mitigation strategies addressing co-existing GEO-NGEO satellite networks. A new approach in the thesis proposes to minimize co-existence interference using MODCOD selection and SS approaches for the optimization of the power spectral density. A decision maker or operator may utilize the recommended optimization approach to trade-off operational parameters and optimum configuration planning under interference

conditions. The thesis's findings may provide insightful information for the community, especially researchers, decision makers, and/or operators, who are concerned in co-existing satellite systems.

The rest of the thesis is structured in the following manner. The interference model and mathematical formulation of the satellite communication link are discussed in Section II. Section III presents the genetic algorithm (GA) and describes the multi-objective optimization problem (MOP) as well as the optimal proposed solutions. In Section IV, the interference mitigation methods' performance is analyzed numerically for comparative assessment. Existing interference mitigation strategies are classified at a high level of quality in Section V, which also covers operational concerns. Section VI concludes with a summary of the main points.

CHAPTER 2

PROBLEM STATEMENT

2.1. Interference Geometry

As the need for low-cost broadband connectivity grows year after year, it is expected that LEO satellites would be used to deliver superior access to people all over the world. The LEO communication topology is presented in Figure 2.1.

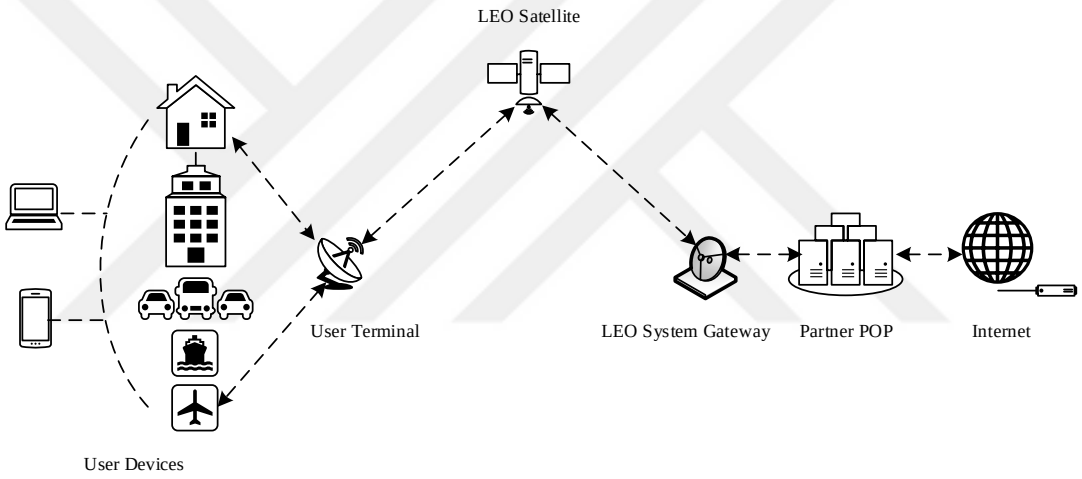

Figure 2.1 LEO Communication Architecture

LEO satellites are launched between 500 and 2000 kilometers above the Earth [1]. Although LEO constellations are in a different orbit than current GEO networks, there is a possibility of interference due to the same communication frequency ranges. As seen in Figure 2.2, in-line interference arises when the LEO satellite moves in the direction wherein the GEO satellite communicates with the GEO earth station.

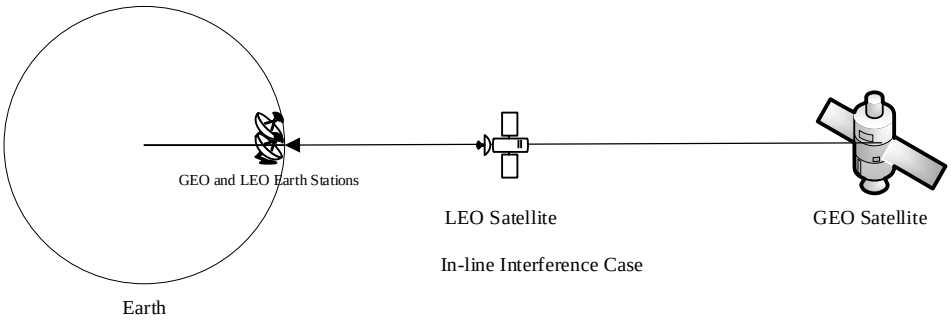

Figure 2.2 The in-line interference scenario among LEO and GEO system

GEO and LEO missions should be kept by a specific angular and operational range so that the two orbits do not interfere with each other. This thesis presents a realistic interference geometry among two different orbits. Downlink interference geometry from LEO system to GEO system is shown in Figure 2.3. The equatorial location of a GEO earth station has been used to establish an EZ for LEO satellites in the recommended interference model. An EA of EZ may therefore be derived mathematically. The plane of the LEO satellite is considered to be the same as the plane of the GEO satellite for modelling interference geometry.

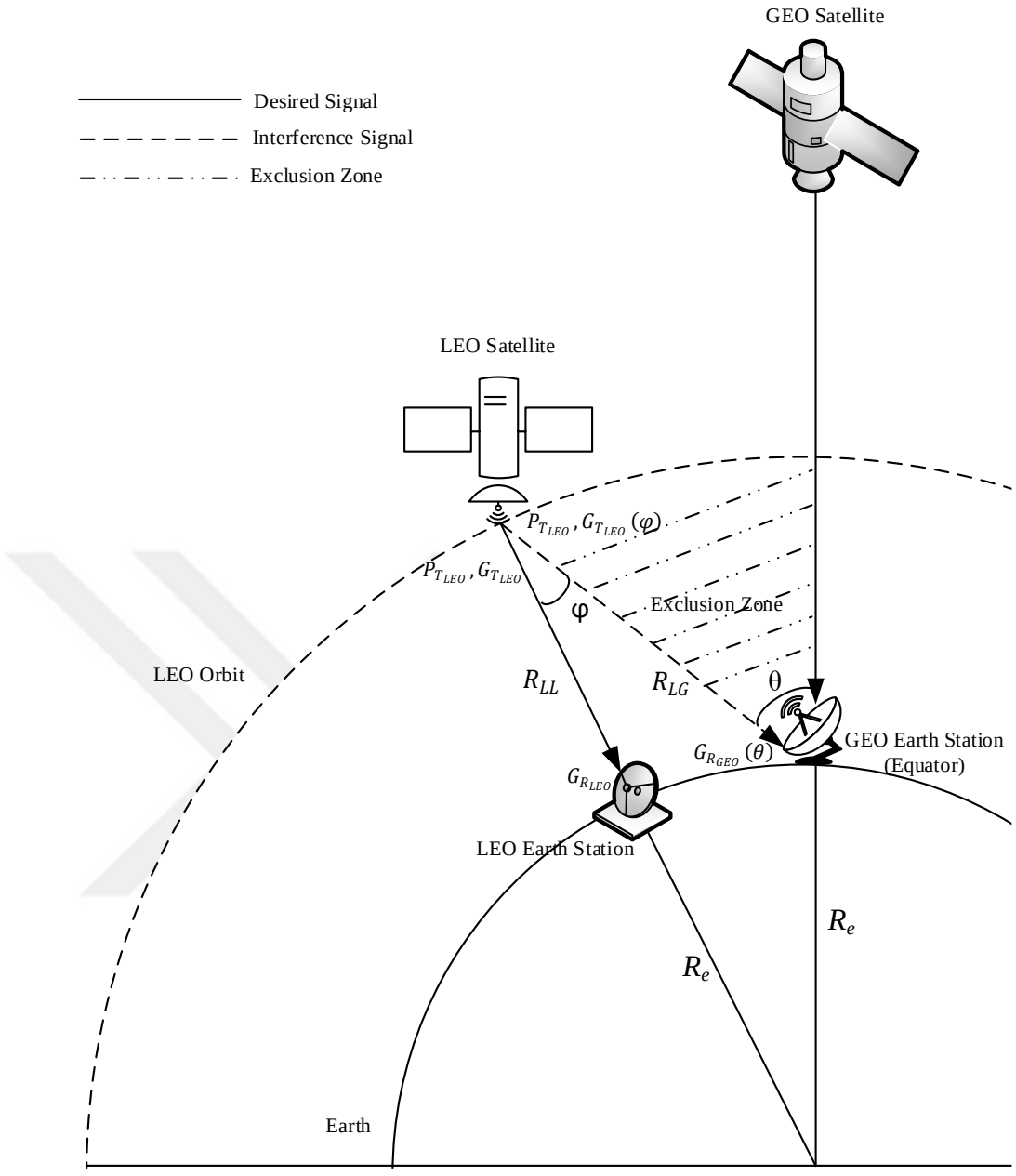

Figure 2.3 The Downlink Interference Model from the LEO to the GEO System

Only 50% of the EZ is shown in the interference geometry, and this should be taken into account when calculating the EA in its entirety.

As illustrated in Figure 2.3, the off-boresight angle of the transmitter or receiver is associated to the antenna position in the propagation direction. Because the satellite's velocity changes the off-boresight angle, the antenna gain changes continuously. the off-boresight angle of LEO transmitter (φ) and the off-boresight angle of GEO earth station (θ) are specified in our model as two distinct angles. Additionally, the (θ) angle

also symbolizes the EA. Because the user's antenna is considered to be tracking the satellite constantly, the required off-axis angle for a LEO user antenna is 0°.

In interference model, the relation between angles may be expressed as follows by using the law of tangents.

$$\frac{R_{LL}}{R_{LL}+2R_e}=\frac{\tan\left(\frac{1}{2}(180-\theta-\varphi)\right)}{\tan\left(\frac{1}{2}(180-\theta+\varphi)\right)} \tag{2.1}$$

where R_e is the radius of the earth and R_{LL} is the distance from the LEO satellite to the LEO earth station. The angle-distance relationship for interference model can be stated as follows using the law of cosines.

$$(R_e+R_{LL})^2 = {R_{LG}}^2 + {R_e}^2 - 2R_{LG}R_e\cos(180-\theta) \tag{2.2}$$

where R_{LG} is the distance from the LEO satellite to the GEO ground station.

To better understand how GEO and NGEO communications interfere with one another, a realistic interference case should be designed. GEO satellite in equatorial orbit with zero inclination angle and standard LEO constellation are considered in this interference case. The LEO constellation does not have steerable beam or steerable antenna technology, nor does it have the capability to communicate with other LEO satellites. LEO satellite also has a restricted ability to mitigate interference with the GEO system, notably in the equatorial zone, by either tilting satellites or turning off communication. This form of constellation is exemplified by OneWeb. As the satellite goes from the mid-latitudes to the lower latitudes, OneWeb utilizes "progressive pitch" model, which tends to give the satellite a bias as it passes [57].

The GEO system is also identified as the primary satellite system. We thus consider the GEO satellite is already operational so the LEO satellite link would be established in the overlapping spectrum with existing GEO network. Because of this, it's necessary to make adjustments to the LEO parameter settings depending on the operational GEO system. The most harmful interference is caused by the downlink interference between

the LEO satellite and the GEO earth station, which is known as co-frequency downlink interference. An LEO satellite operating in the overlapping frequency range as the GEO satellite is assumed for simplicity's sake. It is also expected that the LEO satellite's transmit power density could be changed within a certain range. As it is considered that the satellite-to-earth system distance would stay unchanged, a fixed free space loss is taken into account. All other enviromental effects, including fading due to rainfall, are also neglected for the sake of simplicity in this scenario. All of these simplifying assumptions are performed in order to emphasis on certain critical operational characteristics in the system's best configuration. All of these variables may simply be included into the methodology if required.

2.2. Satellite Communication Link

The architecture of the communication link between the satellite and the end-user is very essential in satellite systems. Figure 2.4 depicts a generic satellite communication network.

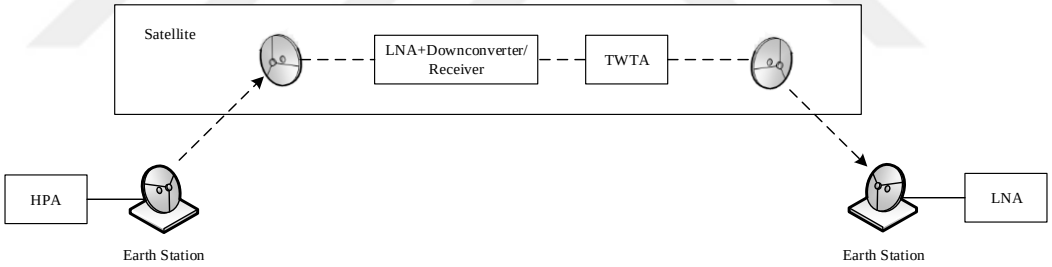

Figure 2.4 The signal path of the satellite communication link

Reliable and continuous data transmission depends on the antenna performance of the receiver and transmitter. The antenna's gain can be calculated using [58]:

$$G = G_0 \left[\frac{J_1(\mu)}{2\mu} + 36 \frac{J_3(\mu)}{\mu^3} \right]^2 \tag{2.3}$$

where $\mu = 2.07123\, sin(\emptyset)/sin(\emptyset_{3dB})$;$J_1$ and J_3 are the first and third order Bessel functions, respectively; $\emptyset$ is the off-boresight angle; $\emptyset_{3dB}$ is the angle related to the

3dB beamwidth; the maximum antenna gain is expressed as G_0 when the off-boresight angle is 0°, and its formulation is:

$$G_0 = \eta \frac{4\pi A}{(\lambda)^2} \tag{2.4}$$

where A represents the antenna area, η is the antenna efficiency, λ is the wavelength.

The Friis transmission equation describes the relationship among transmit and receive power for transmitter and the receiver. The equation for the Friis model is as follows [59]:

$$\frac{P_R}{P_T} = \left(\frac{\lambda}{4\pi R}\right)^2 G_T G_R \tag{2.5}$$

where R is the distance of the link, P_R is the received power, P_T is the transmitted power, G_T and G_R are the transmit and receive antennas gains, respectively. The free space propagation loss FSL accounts for the losses caused by the antenna's spherical scattering. The FSL is a result of transmitter-receiver range and can be computed as follows [59];

$$FSL = \left(\frac{4\pi R}{\lambda}\right)^2 \tag{2.6}$$

Rather than using constant amplitude modulation techniques for satellite communication links, the carrier signal power at the receive side is employed. It is easy to modify the link formulation in this way since the communication link is practically noise-limited.

$$C/N = \frac{P_T G_T G_R}{N}\left(\frac{\lambda}{4\pi R}\right)^2 \tag{2.7}$$

where C is the power of the carrier signal. The noise power is denoted as

$$N = kT_sB \tag{2.8}$$

where k represents the Boltzmann's constant (1.38×10^{-23} W/(Hz · K)), B symbolizes the signal bandwidth and T_s is the receiver's noise temperature. It is also possible express the carrier-to-noise power ratio C/N as follows;

$$C/N = \frac{P_T G_T G_R}{kT_s B}\left(\frac{\lambda}{4\pi R}\right)^2 \tag{2.9}$$

The downlink carrier-to-noise power ratio of the LEO system can be stated as follows using the interference model shown in Figure 2.3 and the C/N formulation earlier

$$C/N_{LEO} = \frac{P_{T_{LEO}} G_{T_{LEO}} G_{R_{LEO}}}{kTB_{LEO}}\left(\frac{\lambda}{4\pi R_{LL}}\right)^2 \tag{2.10}$$

where $P_{T_{LEO}}$ symbolizes the transmit power of the LEO satellite, T is the LEO receiver noise temperature, B_{LEO} represents the LEO signal bandwidth. The transmit and receive antenna gains are symbolized by $G_{T_{LEO}}$ and $G_{R_{LEO}}$, respectively. Using Friis' formulation, interference level of the system I is expressed as;

$$I = P_T G_T G_R \left(\frac{\lambda}{4\pi R}\right)^2 \tag{2.11}$$

Considering a noise-limited link, the interference to noise ratio level I/N can be written as;

$$I/N = \frac{P_T G_T G_R}{kT_s B}\left(\frac{\lambda}{4\pi R}\right)^2 \tag{2.12}$$

The GEO earth station's interference to noise power ratio owing to interference from the LEO satellite can be expressed as follows.

$$\frac{I_{0_{GEO}}}{N_{0_{GEO}}} = \frac{P_{T_{LEO}}}{B_{LEO}} \frac{\lambda^2}{4\pi} \frac{1}{kT} \frac{1}{L_P} \frac{G_{T_{LEO}}(\varphi) G_{R_{GEO}}(\theta)}{4\pi {R_{LG}}^2} \tag{2.13}$$

where $G_{R_{GEO}}(\theta)$ represents the antenna gain pattern of the GEO earth station, $G_{T_{LEO}}(\varphi)$ denotes the antenna gain pattern of the LEO satellite accordingly at the off-

axis on φ and θ planes, and L_P symbolizes the polarization factor. In addition, the following formula can be used to calculate the power flux density (PFD) of an isotropic transmitter [60]

$$PFD = \frac{EIRP(\varphi)}{4\pi R^2} \tag{2.14}$$

where $EIRP(\varphi)$ denotes the effective isotropic radiated power at the off-axis direction of φ angle. Due to the fact that the EIRP might change depending on the direction (for example, if the transmitter did not utilize an isotropic antenna), this term is dependent on the angle, which is also represented here using the symbol φ. As a result, any operating bandwidth of the satellite link can be used to find the effective isotropic radiated power density of LEO satellite ($EIRPD_{LEO}$).

The equivalent power flux-density $EPFD$ is the total of the power flux-densities generated at a reception antenna by all transmitting antennas, taking into consideration the off-axis discrimination of a reference receiving antenna supposed to be oriented in its standard plane. Thus, the $EPFD$ at the reception station can be expressed as follows.

$$EPFD = \frac{EIRP(\varphi)}{4\pi R^2} G_R(\theta) \tag{2.15}$$

where $G_R(\theta)$ symbolizes the reception antenna gain in proportion to the peak receiving gain.

For the multiple interference sources because of LEO satellite systems, the total equivalent power flux density ($EPFD_T$) at the receiving station of the GEO satellite system can be computed as follows [9].

$$EPFD_T = 10log_{10}\left\{\sum_{i=1}^{i=N_a} P_T^i \frac{G_T(\varphi_i)}{4\pi R_i^2}\frac{G_R(\theta_i)}{G_{R_{max}}}\right\} \tag{2.16}$$

where N_a denotes the quantity of the the LEO satellite system's interfering stations which are perceptible from the GEO satellite system's receiving antenna, P_T^i

represents the transmit power of the i-th LEO satellite system's interfering station, $G_T(\varphi_i)$ symbolizes the transmit antenna gain of the i-th LEO satellite system's interfering station while $G_R(\theta_i)$ indicates the receive antenna gain of the GEO satellite system's receiving station in the position of the i-th interfering station of the LEO satellite system, $G_{R_{max}}$ signifies the maximum antenna gain of the GEO satellite system's receiving station, R_i is the distance between the i-th LEO satellite system's interfering station and the GEO satellite system's receiving station.

The total equivalent power flux density ($EPFD_{T_{GEO}}$) can be described in terms of the interference to noise power ratio ($I_{0_{GEO}}/N_{0_{GEO}}$) by combining equations (2.13) and (2.16).

$$EPFD_{T_{GEO}} = 10\log\left[\sum_i \frac{I_{0_{GEO_i}}}{N_{0_{GEO}}} \Big/ \left(\frac{\lambda^2}{4\pi}\,\frac{G_{R_{max}}}{kTL_P}\right)\right] \tag{2.17}$$

The equivalent power flux density for a single entry ($EPFD_{S_{GEO}}$) can be simply calculated [9].

$$EPFD_{S_{GEO}} = \frac{P_{T_{LEO}}}{B_{LEO}}\frac{G_{T_{LEO}}(\varphi)}{4\pi {R_{LG}}^2}\frac{1}{L_P}\frac{G_{R_{GEO}}(\theta)}{G_{R_{max}}} \tag{2.18}$$

2.3. Antenna Radiation Patterns

All types of wireless communications, including satellite networks, are affected by antenna radiation patterns. Since the width of the EZ is extremely dependent on terminal pattern and gain change, it is significantly more essential to pay attention to this. Including the instructions of regulatory authorities [54,55], more realistic patterns are proposed in the interference analysis in this research. Appendix-A and Appendix-B contain the ITU antenna pattern formulation, which is referenced for transmit and receive antennas throughout the research. A paraboloid antenna is expected to be used for both LEO and GEO ground stations, as is the scenario in most other applications.

It is feasible to use curve fitting to describe radiation patterns in compact and mathematically obtainable forms since the ITU recommendation gives extremely specific numerical formulations for the radiation pattern. To achieve the lowest possible error in modeling a data set, curve fitting focuses on the employment of certain functions [61]. Polynomial curve fitting is used in this work. It is possible to use the following curve fitting formula for the LEO satellite system's transmit antenna gain pattern ($G_{T_{LEO}}(\varphi)$)

$$G_{T_{LEO}}(\varphi) = \sum_{n=0}^{U} p_n \varphi^n \tag{2.19}$$

where p_n denotes the polynomial's n-th coefficient, U indicates the polynomial's order. The same method of polynomial fitting can be used to compute the receive antenna gain for the GEO satellite system ($G_{R_{GEO}}(\theta)$).

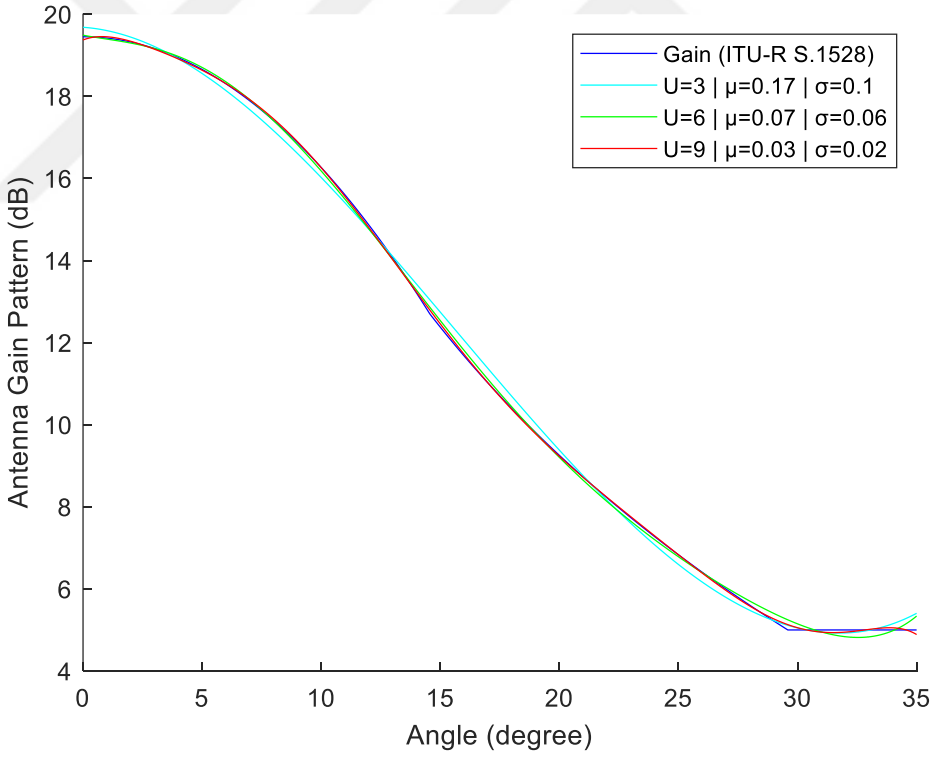

Figure 2.5 Polynomial fitting of the LEO Satellite Antenna Gain Pattern

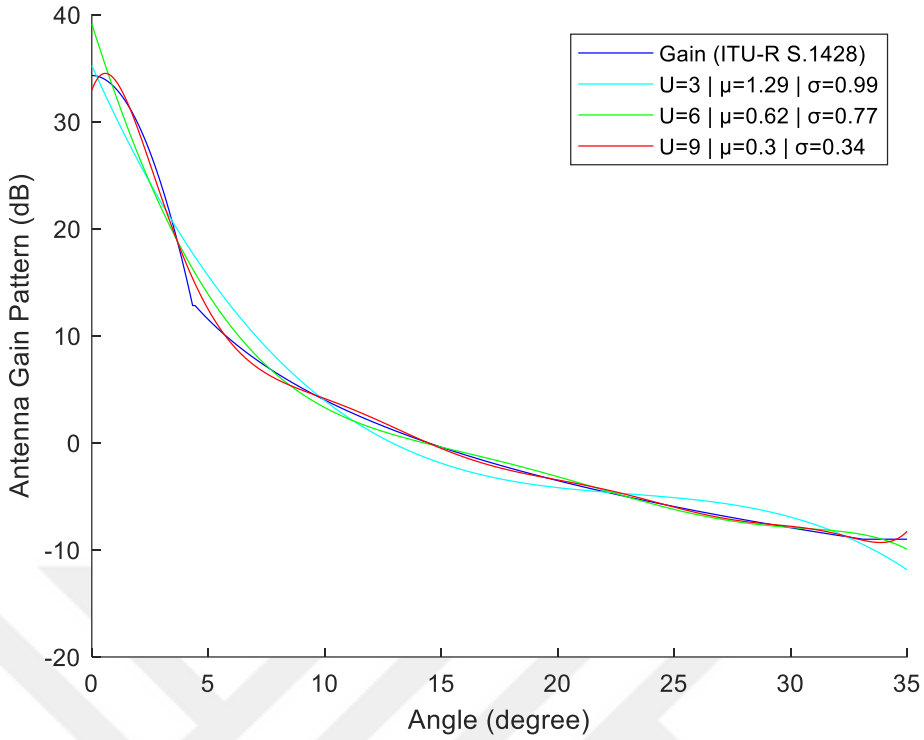

Figure 2.6 Polynomial fitting of LEO-GEO Earth Station's Antenna Gain Pattern

Figure 2.5 and Figure 2.6 show the 3rd, 6th, and 9th order polynomial fits to the transmit and receive antenna gain patterns of the LEO satellite network and the LEO-GEO earth station, respectively. As can be seen in the figures, the errors' mean and standard deviation are computed. It should be noticed that the mean error value in Figure 2.6 (1.29 dB for 3rd order polynomial fitting and 0.3 dB for 9th order polynomial fitting, respectively) is greater than that in Figure 2.5. (0.17 dB for 3rd order polynomial fitting and 0.03 dB for 9th order polynomial fitting, respectively). Assuming that the earth station antennas have well-shaped beams, these results are not unusual. Therefore, the receive antenna gain pattern of the LEO-GEO earth station requires the employment of higher order polynomials, ideally of 9th order. The $[1 \text{ x } (U + 1)]$ vector of polynomial coefficients can be generated using various curve fitting methods and techniques.

2.4. Communication Signalling

2.4.1. Digital Signal

Baseband digital signals, which are having a frequency range of zero to a significant upper limit, as found in source coding communication systems. The analysis of baseband signal qualities may be extended to a variety of characteristics of bandpass signals.

BPSK, QPSK, and M-PSK are the most popular modulation methods in satellite communications. Figure 3 depicts an interference model that takes into account the transmission of a typical LEO system forward link signal. The forward connection employs a Phase-Shift Keying (PSK) signal in accordance with the DVB-S2X standard and performance standards. Aside from these advantages, the DVB-S2X channel type provides a broad range of C/N, which helps to reduce interference and boost capacity at the same time. For LEO or GEO link operation, numerous MODCOD solutions provide more granularity. High-order modulation, in particular, allows much improved spectral efficiency while increasing spectrum utilization.

2.4.2. Communication Channel

Rationally, there should be a maximum amount of symbols that can be communicated per second and yet be retrieved at the receiver for a given channel bandwidth. The received symbol pulses will be spread by a limited channel bandwidth at very high symbol rates because the channel cannot reply at the necessary rate. InterSymbol Interference (ISI), caused by this spreading, prevents the receiver from accurately distinguishing succeeding symbols in a broadcast chain because neighboring symbols in the chain are greatly overlapping.

T_{ts} is the transmission time per symbol, and R_s is the symbol rate, and also the relationship is written as $R_s = 1/T_{ts}$ which is shown also in [62]. In the presence of noise, consecutive symbols may be recognized if the received amplitude of all the other symbols is zero at the instant that the desired pulse is captured.

In the Nyquist theory, a baseband channel is defined as a bandwidth in which transmission is feasible only up to the maximum frequency. A rectangular or "brick-wall" filter characteristic may be used to define such a communication path. This rectangular spectrum has a normalized impulse response that is equal to $f(t) \rightarrow sinc(2\pi tB)$.

At time offsets equal to multiples of $1/2B$ each side of the peak, the sinc function exhibits a characteristic that contains periodical nulls. A band-limited channel's maximum symbol rate with zero interference is determined by $R_s \leq 2B$ which means that the symbol rate cannot exceed double the baseband channel capacity.

An output pulse would oscillate indefinitely if the channel had the 'brick-wall' functionality. Channel filter forms that also meet the Nyquist requirement for zero interference may be found. The Raised-Cosine (RC) spectral shape, whose normalized form is given by [60], is an ideal illustration in communication systems.

$$H(f) = \begin{cases} 1 & if\ 2T_{ts}|f| \leq (1-\alpha) \\ cos^2\left(\frac{\pi T_{ts}}{2\alpha}\left(|f| - \frac{1-\alpha}{2T_{ts}}\right)\right) & if\ (1-\alpha) < 2T_{ts}|f| \leq (1+\alpha) \\ 0 & if\ (1-\alpha) > 2T_{ts}|f| \end{cases} \qquad (2.20)$$

where α is known as the roll-off factor, since the maximum bandwidth filled by the raised-cosine pulse is a criterion $(1+\alpha)$ higher than the comparable Nyquist 'brick-wall' channel filter feature. In the limit $\alpha \rightarrow 0$ the raised-cosine filter drops to the brick-wall filter. The roll-off factor is a range-specific characteristic $0 \leq \alpha \leq 1$.

RC-filtered channel's baseband bandwidth B_{RC} can be described with the Nyquist threshold as [60].

$$R_s \leq \frac{2}{(1+a)} B_{RC} \qquad (2.21)$$

The raised-cosine filter may be approximated rather easily in the real. RC filtering is also typically achieved by providing matching Root Raised-Cosine (RRC) filters at both the transmitter output and receiver input since filtering is usually needed at both the transmitter and receiver. The square root of the required overall RC filter characteristic is produced by the RRC filter.

Baseband signals are multiplied by an unmodulated carrier frequency f_c at the center frequency to produce bandpass signals, which may be considered a pure translation of the baseband signal. Two times as much RF bandwidth is generated as baseband bandwidth. As a result, the IF bandwidth in hertz is equal to two times the baseband signal when a roll-off factor is used, as shown below.

$$B_{IF} = 2B_{RC} = R_s(1 + a) \tag{2.22}$$

Consequently, the LEO forward link bandwidth can be expressed as follows [63]

$$B_{LEO} = \frac{R_b}{m\,r}(1 + \ a) \tag{2.23}$$

where R_b represents the bit rate, r indicates the forward error correction rate (FEC) and m symbolizes the bit rate per symbol for DVB-S2X systems, which incorporates framing overhead.

2.4.3. Spread Spectrum (SS)

In terms of security, spread spectrum (SS) solutions are widely renowned for their ability to withstand interference and jamming. As a result, communications systems use a technology known as Direct-Sequence Spread Spectrum (DSSS). It is based on the principle of decreasing signal strength per unit bandwidth by increasing spectral width by distributing signal power across a much greater spectral range. This research aims to make utilization of the SS's inherent interference resistance.

The user's signal is spread across a broader bandwidth than the symbol rate in the SS. The spreading code is associated to the signal. Multiple correlations, each with a unique symbol latency, are used in a raking spread-spectrum receiver. Multipath impacts can be decreased when they are properly mixed. In the world of wireless communications, SS refers to technologies such as CDM and CDMA. The modulated signal in a SS system is spread across a spectral range that is substantially larger than the bit rate. This spreading factor has the potential to be several orders of magnitude

bigger. Among other features, SS operations are designed to minimize interference to other spectrum users and ensure that only the appropriate receiver can demodulate them. SS is not a modulation technique; rather, it is a way of spreading the bandwidth of a specific modulation scheme. Code division multiplexing (CDM) and code division multiple access (CDMA) are concepts in SS that allow many users to use the same expanded spectrum while still being able to retrieve their content from other transmissions.

Spreading and despreading are two different processes that take place simultaneously. Using a suitable coding sequence, the user's data stream is spread across a considerably wider bandwidth. Spreading the signal power across a considerably wider spectral range results in a reduction in power spectral density. Figure 2.7 illustrates the PSD variation in the DSSS application.

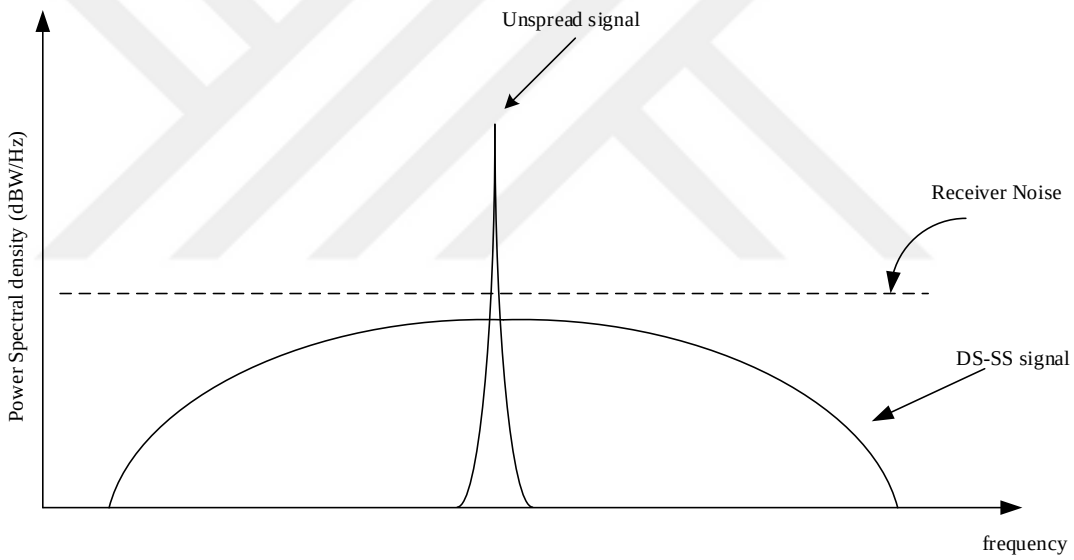

Figure 2.7 Direct-sequency spread-spectrum modulation

Received signals are despread using a code sequence identical to that used to despread the transmitted signal. Even though the despreading procedure has little effect on noise or wideband interference, any narrowband interference is spread, increasing the system's resistance to such interference significantly. Military users place a high value on the SS's higher tolerance to interference and enhanced secure from detection. Narrowband interference resistance enhancement, lower transmission power density, and improved resistance to multipath are just a few of the crucial aspects of SS. In this

study, it is assumed that the LEO communication signal supports the DSSS architecture.

The processing gain G_p of a SS approach is mostly used to describe the methodology. Anti-jamming and interference resistive performance improves as processing gain increases. Spreading factor (*SF*) is a unit that affects the processing gain in DSSS systems with the formulation $G_p = 10\log(SF)$ [64]. The LEO forward link's DSSS signal's bandwidth is calculated by

$$B_{SS_{LEO}} = B_{LEO} G_p \tag{2.24}$$

G_p is expressed as the ratio of the signal bandwidth at input (B_b) to signal bandwidth at output (B_s) [65]. Processing gain G_p is important when analyzing the ability to extract signals from narrowband interference by SS. The processing gain is proportional to the advancement in signal-to-interferer levels.

[66] details the technical specifications for SS applications in forward link. Additionally, [39] discusses the role of SS to the receiving capabilities of next-generation satellite modems in the forward link. SS technology is not yet used with higher MODCODs in modems. Alternatively, it is frequently used in return links. Nevertheless, in our interference model, all MODCODs supporting DVB-S2X are considered to provide SS. In other words, the LEO forward link supports both the DVB-S2X standard and SS. This instance is taken into account in particular since the objective is to determine the effect of SS on creating an ideal EZ.

CHAPTER 3

PROPOSED METHOD

3.1. Multi-objective Optimization Problem (MOP)

In the engineering discipline, multi-objective optimization are well common to solve wide ranges of problems. The objective functions should ideally be optimized simultaneously, but this isn't always possible since the objective functions are in conflict with one another, therefore the optimization process should look for the best possible compromise. Among the major purposes of multi-objective optimization are the preservation of non-dominated points in the objective space and corresponding solution points in the decision space, the continuation of computational development toward the Pareto front in the objective function space, the preservation of diversity of points on the Pareto front and of Pareto optimal solutions, and the provision of a sufficient but constrained quantity of Pareto points for choice by the decision maker. It is possible to formulate a vector function $F(x)$ by optimizing k different objective functions at the same time, and these are known as multi-objective problems [46].

Even while a single optimum solution may exist for a single-objective optimization problem (SOP), the number of possible solutions for multi-objective optimization problems (MOPs) may be available. A multi-objective problem's assessment function, $F : \Omega \rightarrow \Lambda\ (x)$, transfers evaluation criterias $(x = x_1, \dots, x_n)$ to vectors $(y = a_1, \dots, a_k)$. The Pareto Optimality Theory [67] is used to determine the set of possible solutions. Based on the functions and constraints that define the multi-objective problem, this modeling may or may not be onto some portion of the objective function space.

Decisions must be made by picking one or more vectors, each of which represents a solution. Note that the decision makers generally picks a solution from the Pareto front that is suitable to them. Finding a collection of Pareto optimum options is thus critical

to the decision maker's choosing of a settlement solution that meets all of the goals as best it can.

As a result, the MOP is described as the challenge of finding a vector of choice variables that satisfy constraints and optimize a vector function whose components reflect the objective functions. These functions are a mathematical representation of conflicting success criteria. According to a decision maker, the expression "optimize" refers to finding a solution that will satisfy all objective functions [68].

Formulation of A Multi-Objective Optimization Problem (MOP)

Multi-objective optimization is described as the minimizing of the objective function set $F(x)$ subject to the inequality constraints $g_i(x) \leq 0, i = \{1, \dots, m\}$ and the equality constraints $h_j(x) = 0, j = \{1, \dots, p\}$. Multi-objective problems are solved by minimizing the members of a vector F(x), where x is a decision variable vector in n-dimensions from the space Ω. Furthermore, it's worth noting that in order to fulfill an assessment of $F(x)$ in Ω, $g_i(x) \leq 0$ and $h_j(x) = 0$ reflect limitations that must be met while minimizing $F(x)$ [69].

Ideal Vector:

The vector $f_i(x^{0(i)}) = optf_i(x)$ can be expressed with $f_i(x)$ is the ith objective function, and $x^{0(i)} \in \Omega$. Then $f^0 = [f_1^0, f_2^0, \dots \dots, f_k^0]^T$ is the ideal vector for a multi-objective problem, where f_i^0 signifies the ith function's optimum. This means that the ideal vector includes the best possible solution for each individual goal at the same place in R^n.

Pareto Optimality:

A solution $x \in \Omega$ is seen to be Pareto optimum in terms of Ω if or else there is no $x' \in \Omega$ for which $v = F(x') = (f_1(x'), \dots, (f_k(x'))$ dominates $u = F(x) = (f_1(x), \dots, (f_k(x))$. Unless otherwise stated, the term Pareto optimum is interpreted as referring to the whole choice variable space. When it comes to Pareto optimality,

this means that there can't be any possible vector x that will lower one criteria without simultaneously increasing another criterion.

Pareto Optimal Set:

The Pareto Optimal Set, p^*, is expressed as $p^* \coloneqq \{x \in \Omega | \exists x' \in \Omega F(x') \preccurlyeq F(x)\}$. In the decision space, pareto optimum solutions are those options that cannot all be enhanced simultaneously. Non-inferior, acceptable, and effective solutions are all terms used to describe the full set described by p^*. A non-dominated vector is one whose associated vector is not dominant. Pareto optimum solutions and decision variables may be implicitly identified by picking a vector from this vector set. The Pareto optimum set may have no obvious connection between these options. All solutions with non-dominated related vectors are included in this set. The assessed functional values of Pareto optimum solutions classify them.

Pareto Front:

The Pareto front pF^* is formulized as $pF^* \coloneqq \{u = F(x) | x \in p^*\}$. Non-dominated vectors are generally termed as the Pareto front when plotted in the objective space. Non-dominant objective vectors are the result of assessing every feasible solution in Ω and forming a set of non-dominated objective vectors known as pF^*. A line or area mathematical statement that comprises these points is difficult to find, and in many circumstances, it is unachievable. Numerous points in and their associated $f(\Omega)$ are often used to build the Pareto front. Identifying the non-dominant points and building the Pareto front are achievable when there are enough of them. Figure 3.1 is an example of a Pareto front.

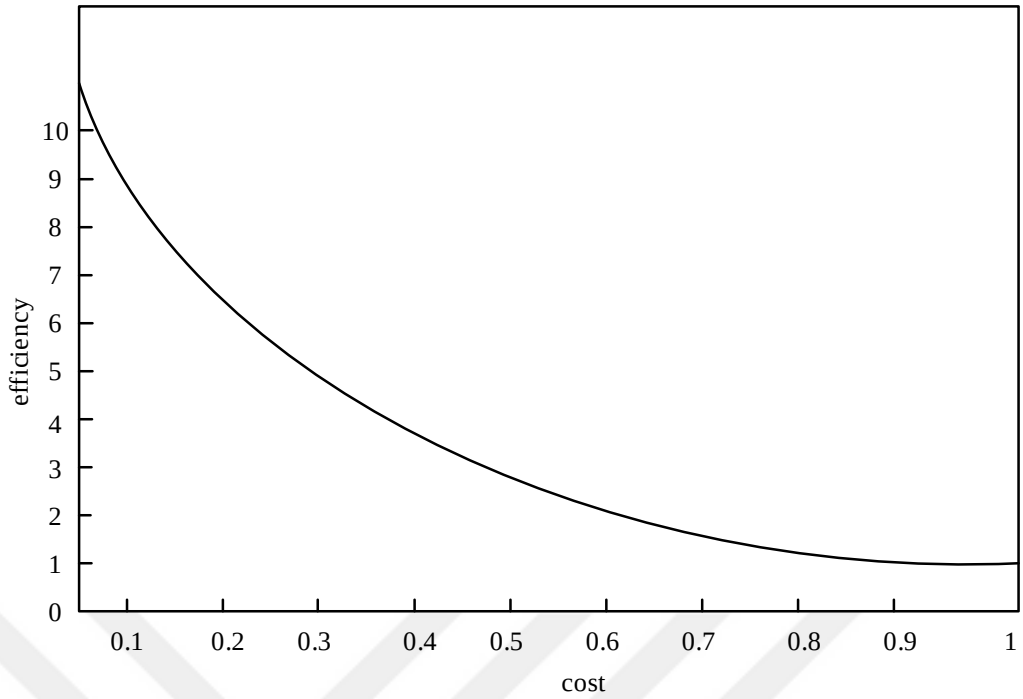

Figure 3.1 Pareto front of a cost-efficiency problem

3.2. Multi-objective Genetic Algorithm (MOGA)

Optimizing methods in the literature include the direct technique, gradient-based, geometric modeling, and genetic algorithms (GA), among other options. The GA, a population-based approach, can handle MOPs effectively [48], despite the difficulty of finding solutions for the selection. These preferences may be taken into consideration by this solver when selecting the optimum solution [49]. Employing pareto frontiers, this approach is successful in solving MOPs [50]. Multi-objective optimization and GA may both benefit from the Pareto front approach [51], which can be used as a reference technique to include preferences.

GA is a product of living beings' evolutionary systems. GA optimization provides a number of benefits over standard algorithmic optimization techniques. Non-linear problems may be solved using GA, and it does not need differential evolution. When attempting to minimize or maximize the issue, GA optimization provides a global solution. GA optimization is a good fit for this kind of issue because of these characteristics.

Precise and reliable Pareto front detection is guaranteed using MOGA approach. As a result of this high number of repetitions, the MOGA approach is not ideal for finding the Pareto front in a fast and efficient manner. The GA's crossover operator may take advantage of structures that are excellent for multiple goals. There's no need to prioritize, scale, or weight goals in a MOGA problem. To solve MOPs, the GA is one of the most common evolutionary algorithms.

Based on Darwin's theory of evolution by natural selection, MOGA's evolutionary algorithms use evolutionary principles. In this type of approach, the design specifications constitute a 'genetic string,' similar to DNA in a biological system, which uniquely encodes each design point in a randomly chosen population in dimensional space. This is followed by a series of iterations where the population's appropriate design points are deemed to be the most "fit" and permitted to live and reproduce. Using mathematical equivalents of natural selection, crossover and mutation, the program models the evolutionary process. An optimal design point is found that minimizes the problem's overall objective function.

Many researches employ GA to optimize system parameters. Figure 3.2 depicts the GA optimization workflows. It is at this stage that first populations are generated. Constraints are followed in the selection of main populations. Using each chromosome, the fittest is evaluated and the findings ranked. Then, the chromosomes that have been assessed are selected to generate a new generation based on their fitness. The constraint-dependent selection strategy is used in this work, which is one of various theoretical options. The technique guarantees that the population is diverse enough to avoid inadequate immature solutions. Once the best parent has been determined, the crossover process may begin. Using the crossover, chromosomes may be swapped out to generate a new generation of descendants. Then, during the mutation stage, chromosomes begin to randomly mutate. In both crossover and mutation, system factors are taken into consideration. Until the specified termination requirements are met, all processes are carried out in a continuous manner. In [46,49], readers may get more information on GA and its verification and validation.

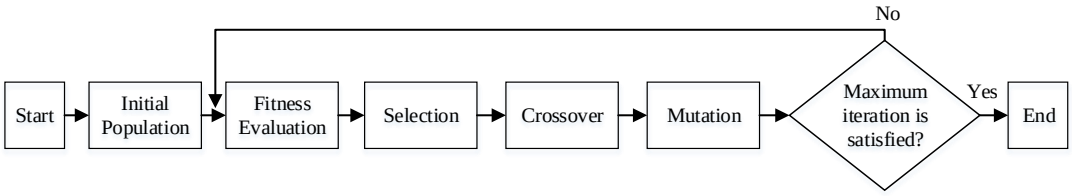

Figure 3.2 Genetic Algorithm Flowchart

Various regions of a solution space are simultaneously searched by Genetic algorithm (GA) techniques. Despite the fact that GA requires a large computational effort, users do not need to prioritize, scale, or weight any of the processes involved in the algorithm. In the thesis study, an evolutionary algorithm, i.e. genetic algorithm (GA), based on the theory of survival of the fittest is preferred for the optimization problem solution.

3.3. Estimation of the Optimal Exclusion Zone (EZ) with SILA Technique

The SILA technique, which combines spatial isolation and link adaptation, is proposed in this research for the interference mitigation. The GA was employed as the optimization strategy in the proposed SILA technique. Figure 2.3's geometry shows that the EZ may be optimized by adjusting the EA (θ). The EZ becomes smaller as the EA decreases. If the assigned bandwidth can be modified to match the operating parameters of the LEO satellite system, then this should be able to be done. In terms of competing priorities, the EA and allocated bandwidth are two significant considerations to evaluate. The contradictory goals must be addressed in accordance with the interference-limited performance criteria for the LEO satellite network, i.e., other operating parameters of both LEO and GEO should be restricted.

The MOP is a feasible option when many goals are at odds with one another. All conceivable trade-offs among opposing goals are represented by the MOP solution set. As a result, the most ideal option will be the one that most aligns with the goals at hand. This collection of solutions is referred to as the Pareto optimal set, as previously mentioned. In order to arrive at a Pareto optimal set, MOP solutions seek to find optimal solutions. The term "best-performing" or "non-dominant solution set" both refer to this set. The suggested MOP is based on the trade-off line between both the EA and the allocated bandwidth in Figure 2.3, which illustrates the issue of

interference among LEO and GEO networks. Using MODCOD configurations in the developed framework, power spectral density will be the main criterion for a desired data rate and all other restrictions. Pareto front set founded on MOP solution under various operation conditions gives alternate possibilities to the decision makers. Additionally, this might increase system interoperability and boost the efficiency of the system resources.

EA (θ) and allocated bandwidth (B_{LEO}) have been determined in the preceding chapter using system operating data. It's also possible to get information on the single-entry equivalent power flux density $\left(EPFD_{S_{GEO}}\right)$, the downlink carrier to noise ratio of the LEO system (C/N_{LEO}), and effective isotropic radiated power flux density ($EIRPD_{LEO}$). As a result, we may frame the following multi-objective optimization problem:

$$
\begin{aligned}
& \textit{Minimize exclusive angle (EA) } (\theta) \\
& \textit{Minimize } B_{LEO} \\
\text{s.t. C.1.} \quad & EPFD_{S_{GEO}} \leq EPFD_{S_{GEO_{th}}} \\
\text{C.2.} \quad & B_{LEO} \leq B_{LEO_{max}} \\
\text{C.3.} \quad & C/N_{LEO} \geq C/N_{LEO_{th}} \\
\text{C.4.} \quad & EIRPD_{LEO} \leq EIRPD_{LEO_{max}}
\end{aligned}
\tag{3.1}
$$

where th denotes the lowest value and max denotes the highest value. In addition, C.1 is to minimize interference with the GEO ground station, C.2 is to ensure that the LEO transmitted BW does not exceed the maximum allowable $B_{LEO_{max}}$, C.3 is to keep the acceptable C/N on the LEO link, and C.4 is to manage the LEO satellite system's EIRP density level. Owing to the intricacy of the objective functions and the complexity of the constraints, the optimization convention is not employed in this problem.

Two distinct operational cases are examined for addressing the optimization problem in equation (3.1). For Case-1, the proposed solution does not employ SS, but for Case-2 the proposed solution does make utilisation SS. In Case 1, MOP has been performed by looking for the optimum MODCODs of the LEO communication link based on the LEO transmitter's off-boresight angle (φ), which controls the EA (θ). That is to say, the power spectral density is optimized in order to achieve the optimal bandwidth and

EZ allocation for the desired data rate. MODCODs are given in the search area for the DVB-S2X standard, which is anticipated to be supported by the LEO forward link transmission network. Within the 0° to 20° range, the off-boresight angle of the LEO transmitter (φ) is taken into consideration. Spread spectrum (SS) and MODCOD search strategy are used in Case 2 to improve the power spectral density, resulting in an SF of up to 8. Table 3.1 shows the multi-objective problem in a table style.

Table 3.1 Multi-objective Optimization Problem Formulation for SILA Technique

Functions	***Constraints***	***Bounds*** ***Case-1*** ***(Case-2)***	***Notes***
$min\, B_{LEO}$	$EPFD_{S_{GEO}} \leq EPFD_{S_{GEO_{th}}}$	$\mathrm{DVB-S2X}$	*Acc. to ITU, the GEO earth station's maximum EPFD acceptability limitation is* $-160\ dB(W/m^2)$ *for the 60 cm satellite dish.*
$min\, \theta$	$B_{LEO} \leq B_{LEO_{max}}$	$0 \leq\ \varphi \leq 20$	*The LEO forward link's maximum channel bandwidth is 250 MHz.*
	$C/N_{LEO} \geq C/N_{LEO_{th}}$	$(1 \leq SF \leq 8)$	*The* $C/N_{LEO_{th}}$ *ratio is employed based on ETSI simulations of DVB-S2X.*
	$EIRPD_{LEO}$ $\leq EIRPD_{LEO_{max}}$		*The LEO system in Ku-Band has a maximum* $EIRPD_{LEO_{max}}$ *value of* $-13.4\ dBW/4\ KHz.$

Table 3.2 lists the GA optimization settings for the multi-objective optimization problem.

Table 3.2 GA Optimization Settings for the MOP

Parameter	Value
Population Type	Double vector
Population Size	1000
Crossover Function	Intermediate
Crossover Rate	1.0
Mutation Function	Constraint dependent
Reproduction	0.8
Selection Function	Tournament
Number of individuals	350

Table 3.3 lists the specifications of the LEO and GEO satellite systems that are used to solve the multi-objective optimization problem.

Table 3.3 Parameters of the LEO and GEO Systems

Parameter	***LEO Satellite***	***LEO Earth Station***	***GEO Satellite***	***GEO Earth Station***
Satellite	Typical LEO Constellation		Reference GEO Satellite	
Altitude	1200 km		35786 km	
Location				Equator region
Antenna radiation pattern	ITU-R S.1528	ITU-R S.1428		ITU-R S.1428
Antenna diameter	0.1 meter	0.6 meter		0.6 meter
Antenna gain	19. 45 dBi	34.31 dBi		34.31 dBi
Transmit power	$0.001 \leq P_{T_{LEO}} \leq 20$ W for Sec.4.2 $7.079 \leq P_{T_{LEO}} \leq 14.125$ W for Sec.4.3			
Maximum downlink EIRP density	-13.4 dBW/4 KHz			
Carrier frequency	10.7 GHz		10.7 GHz	
Reference bandwidth				40 KHz
EPFD limits				-160 dB(W/m^2)
The LEO forward link's maximum assignable bandwidth		250 MHz		
Noise temperature		275 K		
Modulation standart		DVB-S2X		
Spreading factor		1 to 8		
Roll-off		0.2		
Polarization factor		1		

For practical purposes, conventional parameters are employed in the problem solution. Interference between different satellite systems and ground stations may be assessed using this approach. The recommended multi-objective optimization method may therefore be used in a similar way to that scenario.

In order to solve the MOP, GA has been used and the findings are shown in Figure 3.3 and Figure 3.4. The pareto front shows the trade-off between the LEO link operating condition (MODCOD and the allocated bandwidth) and the EA for operational transmission bit rates of 100 Mbps and 200 Mbps. There is a spread spectrum (Case-1) and a non-spread-spectrum (Case-2) option for each data rate.

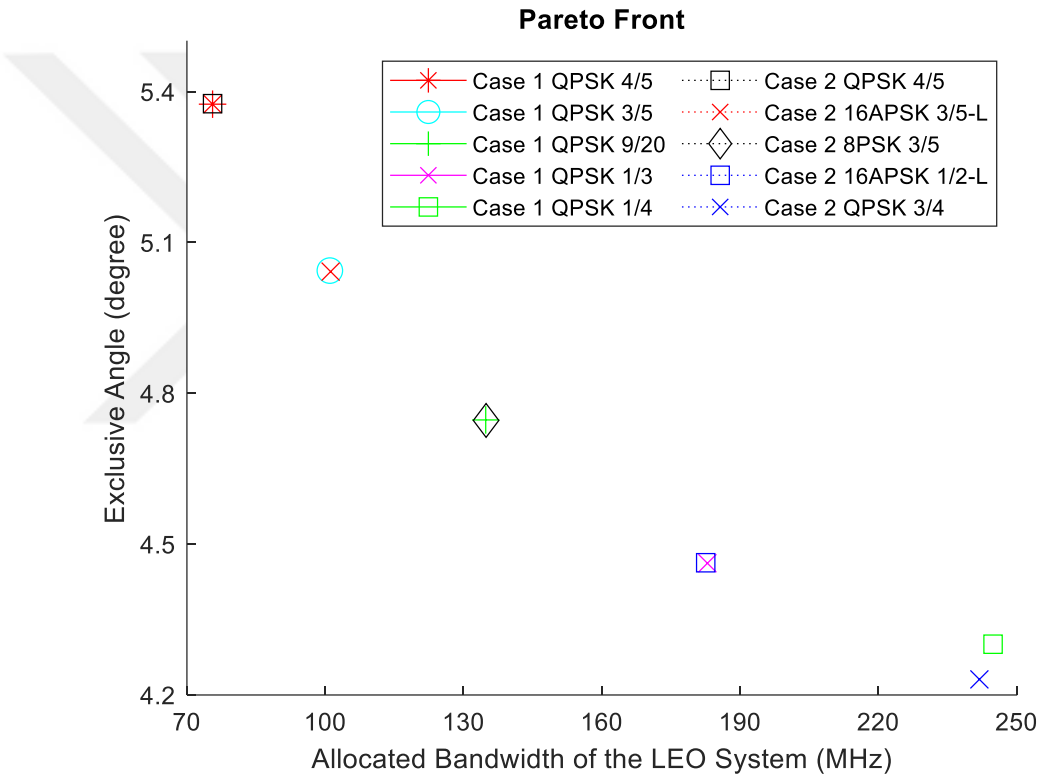

Figure 3.3 Optimal Parameters for 100 Mbps Transmission Rate

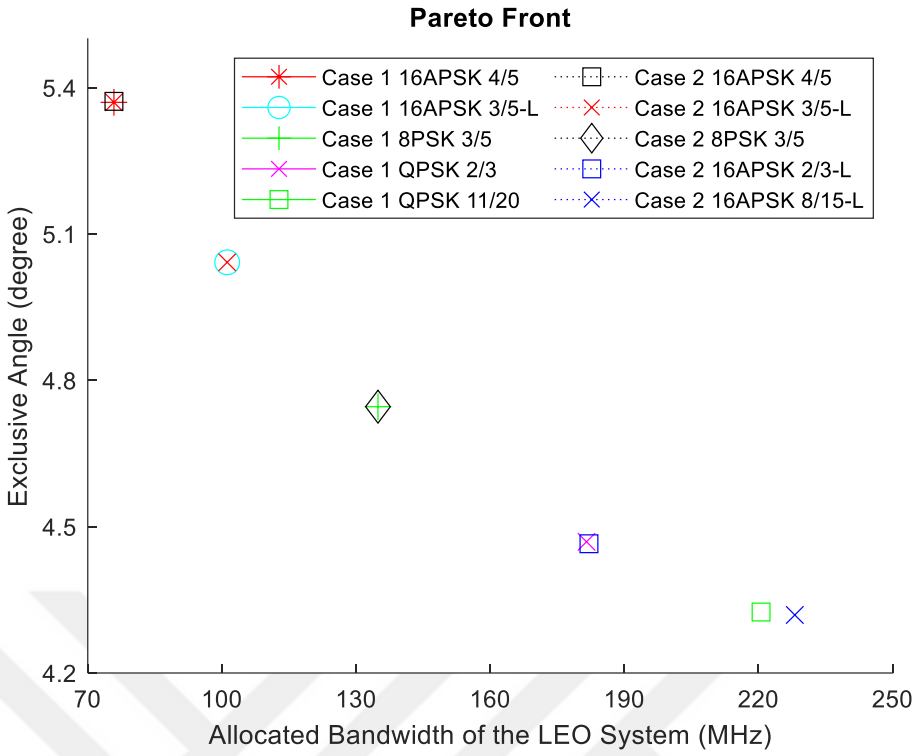

Figure 3.4 Optimal Parameters for 200 Mbps Transmission Rate

On the pareto front, a variety of dominating solutions and a high degree of diversity are observable. A decision-maker or a satellite operator might benefit from this versatility in satellite operation. Typically, the EA is higher when bandwidth allocations are lower. To be clear, the EA does not change linearly with bandwidth allocation as per ideal MODCODs. The MODCOD appears to be independent of the spreading factor at the maximum EA, when the allocated bandwidth is lowest. On the other hand, when it comes to selecting various MODCODs, the spreading factor (SF) is crucial. Nevertheless, with a transmission bit rate of 200 Mbps, the impact of SF appears to be substantially reduced. There are two options: lower MODCODs utilization or implementation spread spectrum (SS) for the LEO system. The operator has the ability to pick the most suitable MODCODs and other operational settings by choosing the EA and the assigned bandwidth. Using a bandwidth of ~220/242 MHz, the operator may take advantage of the lowest feasible EA (~4.2/4.3 degrees) between the GEO and LEO networks. In other expressions, the higher the bandwidth assigned, the lower the EZ where the LEO satellite is not allowed to operate. In this case, the MODCODs and SFs only offer additional power spectral density utilization options.

QPSK 1/4 and QPSK 3/4 for 100 Mbps, and QPSK 11/20 and 16APSK-8/15-L for 200 Mbps, are the MODCOD for the lowest EA where the assigned bandwidth is the highest for Case-1 and Case-2, respectively. A MODCOD with an EA of 4.75° and a bandwidth of 135 MHz might be either 8PSK-3/5 or QPSK-9/20.

For Case 1, the MODCODs shift from QPSK 1/4 at the lowest exclusive range to QPSK 4/5 at the maximum EA when the transmitted data rate is 100 Mbps. For Case 2, it shifts from QPSK 3/4 to 4/5. When the transmitted data rate is raised to 200 Mbps, the MODCOD generally shifts from QPSK to APSK. Based on the transmitted bit rate, we may deduce that the operator can analyze the service requirements for an EA.

Table 3.4 describes the optimum solution's boundary conditions in SILA technique. At data rates of 100 Mbps and 200 Mbps, it is demonstrated that the EA can be lowered by up to 21.3% and 19.6%, respectively, from the initial anchor point.

Table 3.4 An Overview of the Optimal Solutions

Exclusive Angle (EA) Results for Case-1 (Case-2)			
Bit rate (Mbps)	Initial Anchor Point	Final Anchor Point	Reduction (%)
100	5.38 (5.38)	4.30 (4.23)	20.0% (21.3%)
200	5.37 (5.37)	4.33 (4.32)	19.5% (19.6%)

The optimization problem proposed in the thesis is solved one time with a spesific resolution and optimal solution set is obtained. Since the optimization algorithm's conditions and bounds are specified in line with realistic cases and an inclusive approach, obtained results are also applicable to a wide range of practical scenarios. In this case, as the resolution of the GA is extremely high, the precision of the obtained results increases proportionally. As long as the problem conditions do not change, acquired typical results can be executed properly. In the event that the system

conditions change, for instance if a different LEO system is chosen for interference evaluation, it is advisable to rerun the optimization algorithm using the new LEO system parameters. Since the optimization problem is defined in a compact structure, it will not be difficult to solve the problem and obtain new practical results. From this point of view, it can be said that the proposed method brings advantages in terms of practical application in the field.

For satellite communications, SS methods are more often utilized on the return link instead of the forward link. As a result of this research, it has been shown that using SS methods on forward links with higher MODCODs may help to lower the EZ and increase operational versatility. The EZ may be lowered progressively, but the EPFD limit should be determined in accordance with the regulatory organizational boundaries (ITU). However, if this limitation is surpassed, the LEO system is going to make an effort higher than predicted EPFD, which indicates that it might potentially interfere with GEO network.

The bandwidth allocation alternatives of LEO communication link are shown in the optimal configuration when distinct DVB-S2X MODCOD configurations are applied individually in the LEO communication link. It is clear that the pareto front gives comprehensive data about the trade-off among two goals, allowing the decision-maker or operator to alter the design settings of the communication link as needed. Using appropriate LEO communication link settings, SILA technique limits EZ, proving its viability and high performance. As a result of the recommended optimization technique, system resources may be fully exploited while preserving the communication link. A more flexible technique for interference mitigation may be obtained if the DVB-S2 ACM [38] is employed in the LEO communication link. In order to optimize the given bandwidth and EZ without interrupting the communication link, the ACM contribution allows the MODCOD to be adjusted during the operation. Existing mitigation approaches may be used more effectively, as well as a proposed optimization strategy, to lessen the amount of interference among two networks. As a last step, various current beamhopping and adaptive power control algorithms [18,19] may be combined to further enhance the system performance. When employed in SILA, MODCOD selection and SS allow for more resource flexibility, which helps

with flexible resource distribution. This study's new technique may be used to next-generation satellites as well.

CHAPTER 4

COMPARATIVE ASSESSMENT OF INTERFERENCE MITIGATION TECHNIQUES

In this section, studies have been carried out to compare the differences between the proposed SILA technique based on the thesis study and other approaches in the literature. For this purpose, it is aimed to reveal the contribution to the literature in more detail by examining the benefits of the work done within the thesis. Qualitative evaluation and quantitative measurement-based methods has been used to compare the SILA technique with existing studies. In this context, differences, advantages and disadvantages has been revealed by making both quantitative and qualitative approach-based comparisons. In addition, it has been shown that performance improvement can be achieved by using different methods together in quantitative evaluation.

When it is desired to compare the SILA method with the existing studies using quantitative measurement methods, there are differences among the proposed solutions in terms of the problem definition such as frequency band, interference geometries, satellite and ground station locations, link calculation parameters, satellite platforms and satellite positions. Therefore, it has been determined that there are major differences in the problem input parameters for the solutions presented with different methods. Therefore, it has been evaluated that it may not be possible to obtain healthy results in this way by directly comparing the differences in the system input variables by taking the results of one-to-one study specific to any criterion. On the other hand, since the system input parameters are independent of each other, it is not possible to present a scientifically direct proportional or numerical comparison between the results obtained at the system output. Another point here is that the existing studies only provide simulation-based statistical information and do not contain numerical data similar to proposed SILA technique results. Therefore, during detailed analyses for the quantitative comparison, the approaches in the existing studies has been

examined in detail, and the main differences between other problem conditions and our problem definition with SILA technique has been revealed. Then, based on these different methods presented in other studies, different approaches and basic input parameters has been also determined. In addition, a comparative process has been made with reference to other parameters that are considered to be common between these different approach parameters and our SILA technique.

For this purpose, the major and critical parameters of the current studies in the literature has been determined. Then, it is evaluated that it would be appropriate to compare these parameters with our approach presented with SILA technique, which is the main criteria of our problem solution. The fact that they are concerned with communication link conditions and spatial characteristics of the system, as opposed to other interference mitigation techniques, makes the Power Control (PC) [7,16,19,22], spatial isolation (SI) [3,8,11], and SILA [12] approaches comparable to one another. Considering the biggest differences between these studies and our solution approach with SILA, SILA technique presents an optimization algorithm based on power spectral density, while current studies adopt only PC or SI methods for the interference mitigation strategy. In other words, PC and SI techniques have adopted only a PC or SI-based approaches instead of considering optimal bandwidth use, optimal modcode selection or spread spectrum (SS) technique for solving the interference mitigation problem. In these studies, it is aimed to protect the simultaneous link quality while trying to minimize the interference risk of the two systems. For a a quantitative-based comparison methodology SI and PC-based interference mitigation approaches, which is taken as the basic criterion in other problems, is applied specifically to our problem conditions, and the results are compared with SILA results.

4.1. Performance Analyses of SI and SILA Techniques

In this section, quantitative-based comparative analyzes has been performed between the SI technique [3,8,11] and the SILA [12] technique within the scope of the thesis. In SI techniques, an EZ is defined in the interference model and LEO satellites are not allowed transmition in this region. This EZ is represented by the EA within the

interference geometry. On the other hand, in the SILA technique, EZ is defined with a different perspective under certain interference conditions. The biggest difference here is that the optimization of link parameters is also recommended to minimize the EZ in the SILA technique. In order to compare both interference mitigation methods on a quantitative basis, evaluation was made under similar interference conditions. In this context, the interference conditions proposed in the thesis has been taken into account. The details of the interference parameters considered for the comparative assessment are given in Table 3.3.

By using the interference conditions within the scope of the thesis, EA analysis according to the highest modcodes that can be obtained in SI approach and SILA techniques (Method-1) and minimum EA values that can be obtained with the MODCOD selection via link optimization (Method-2) in SILA technique are evaluated in Table 4.1.

Table 4.1 Exclusive Angle (EA) Evaluation for SI and SILA Techniques

	SI Technique		SILA Technique Method-1 (Method-2)		Comparative Assessment
Bit rate Mbps	Allocated MODCOD	Calculated EA degree	Allocated MODCOD	Calculated EA degree	Reduction in the EA
100 Mbps	QPSK 4/5 (QPSK 4/5)	23.98 (23.98)	QPSK 4/5 (QPSK 1/4)	5.38 (4.30)	77.6% (82.1%)
200 Mbps	16 APSK 4/5 (16 APSK 4/5)	23.98 (23.98)	16 APSK 4/5 (QPSK 11/20)	5.37 (4.33)	77.6% (81.4%)

When the results are examined, the EA can be reduced by 77.6% in 100 Mbps transmission rate for the same MODCOD selection by using the SILA technique. With MODCOD optimization, the EA can be also reduced up to 82.1%. For the comparative assessment of 200 Mbps data rate, the EA can be reduced by 77.6% for the same MODCOD selection and it can be also reduced up to 81.4% with MODCOD

optimization. The obtained comparative results are presented in the Figure 4.1 below, along with the bandwidth assignment.

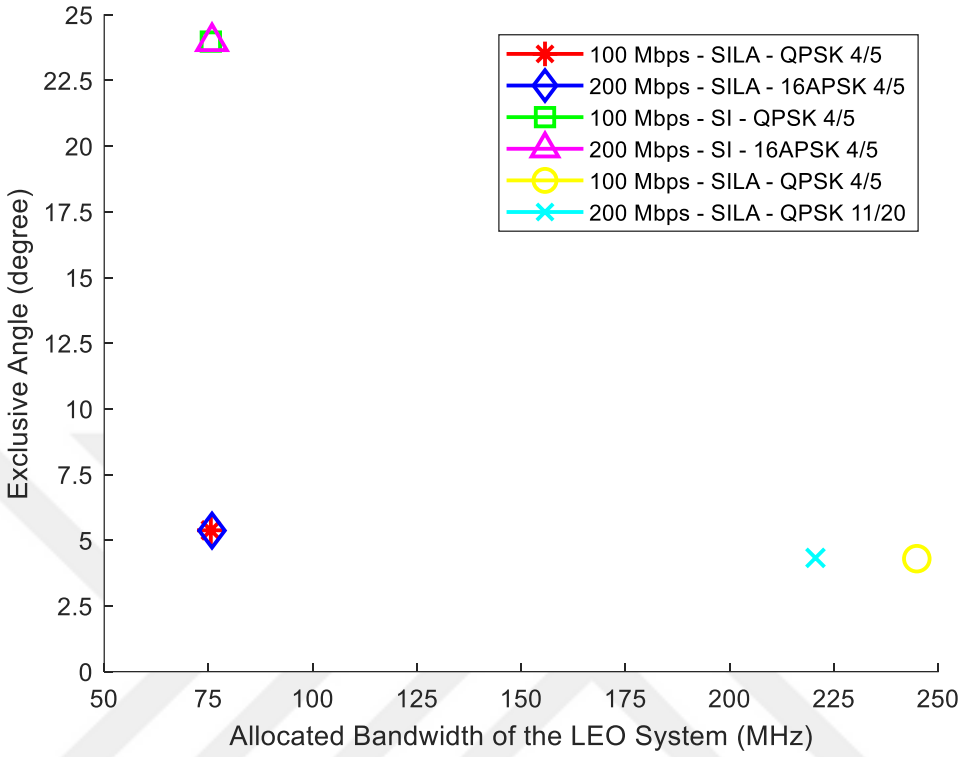

Figure 4.1 EA and Bandwidth Allocation Ranges for SILA and SI Techniques

When we analyse obtained results, the EA assignment using the SI technique brings a higher EZ necessity. This situation also increases the turn-off time of LEO satellites. In the SILA technique, under similar interference conditions (Method-1), a significant reduction of the EA can be achieved with the proposed approach. In addition, EA can be reduced more with the PSD optimization (Method-2) in SILA technique. In this way, co-existence interference for LEO-GEO satellites can be minimized while providing the link quality requirements. As a result, it is shown that a more efficient planning can be made in constellation by significantly shortening the turn-off time of LEO satellites.

4.2. Comparative Evaluation of Power Control (PC) and SILA Techniques

Similar operating conditions and system parameters should be taken into account when comparing various interference mitigation strategies. Using this method, a comparable data set may be obtained for assessment purposes. Consequently, Chapter II's interference model is employed as the framework for quantitative assessment. Comparative study of PC and SILA approaches is carried out utilizing the interference geometry given in Section 2.1 of this study. Both approaches may be used with the interference model mentioned in the comparison assessment, which is the primary factor in favor of these two strategies. Due to the problem-solving technique in the interference model provided in this study, the application of additional interference models experiences challenges. If an interference model and system characteristics are properly defined, this may be expanded to other interference mitigation methodologies.

It is the target of both PC and SILA strategies to reduce the co-existing interference between NGEO and GEO systems while concurrently preserving the service quality of the NGEO system. When it comes to the execution of these interference mitigation strategies for reducing co-existing interference, however, there are substantial variations between the two approaches. Considering that the NGEO system has a limited power, it is essential to minimize its transmit power in the PC method [7,16,19,22] in order to achieve effective interference mitigation. Contrary, the SILA approach aims to employ the optimal bandwidth assignment by concentrating on the power spectral density function rather than the power function.

Section II's interference model is used to develop a power control-based optimization problem. $P_{T_{LEO}}$ is specified as an objective function in the PC approach since the goal is to reduce the power of the NGEO transmitter. The SOP is then used to define the optimization problem. In the optimization algorithm, it is preferred to use an evolutionary algorithm, also known as a genetic algorithm (GA), which is based on the idea of survival of the fittest [12]. It is thus possible to establish the optimization problem for the PC-based interference mitigation methodology as

$$\begin{aligned} &\textit{Minimize power } P_{T_{LEO}} \\ \text{s.t. C.1.} \quad & C/N_{LEO} \geq C/N_{LEO_{th}} \\ \text{C.2.} \quad & EPFD_{S_{GEO}} \leq EPFD_{S_{GEO_{th}}} \\ \text{C.3.} \quad & B_{LEO} \leq B_{LEO_{max}} \end{aligned} \tag{4.1}$$

where " th " indicates the threshold value and " max " indicates the maximum value of relevant parameters. Additionally, C.1 is assigned to keep the appropriate C/N ratio on the LEO link, while C.2 is assigned to minimize interference with the GEO ground station. C.3 is assigned to ensure that the LEO transmission bandwidth does not exceed the allowable maximum bandwidth $B_{LEO_{max}}$. Table 4.2 lists the constraints, lower and upper limits of the optimization problem.

Table 4.2 Optimization Problem Formulation for PC Technique

Function	***Constraints***	***Bounds***	***Notes***
$min\ P_{T_{LEO}}$	$C/N_{LEO} \geq C/N_{LEO_{th}}$	$0 \leq \varphi \leq 20$	*Acc. to ITU, the GEO earth station's maximum EPFD acceptability limitation is* $-160\ dB(W/m^2)$ *for the 60 cm satellite dish.*
	$EPFD_{S_{GEO}} \leq EPFD_{S_{GEO_{th}}}$	$0.001 \leq P_{T_{LEO}} \leq 20$	*The LEO transmit power range is 0.001 mW to 20 W.*
	$B_{LEO} \leq B_{LEO_{max}}$		*The* $C/N_{LEO_{th}}$ *ratio is employed based on ETSI simulations of DVB-S2X.*
			The LEO forward link's maximum channel bandwidth is 250 MHz.

Table 3.3 also lists the characteristics of the LEO and GEO satellite systems that are used to solve the optimization problem. For 100 and 200 Mbit transmission rates, the problem solution yields the optimal power, bandwidth, MODCOD, and EA values. Table 4.3 lists the SOP parameters that are typically configured using the PC method.

Table 4.3 Parameter Optimization for PC Technique

Bit rate (Mbps)	Optimized Power $P_{T_{LEO}}$ (W)	Allocated MODCOD	Allocated BW (MHz)	Calculated EA (degree)
100	0.90	QPSK 1/3	182.93	13.10
200	1.97	QPSK 1/2	242.91	9.52

Every generation yields the population's "best and mean values" when using GA-based SOP methodology. After a set number of iterations, the best fitness value is achieved. Transmission rates of 100 Mbps and 200 Mbps have been used to calculate the fitness values of power as shown in Figure 4.2 and Figure 4.3.

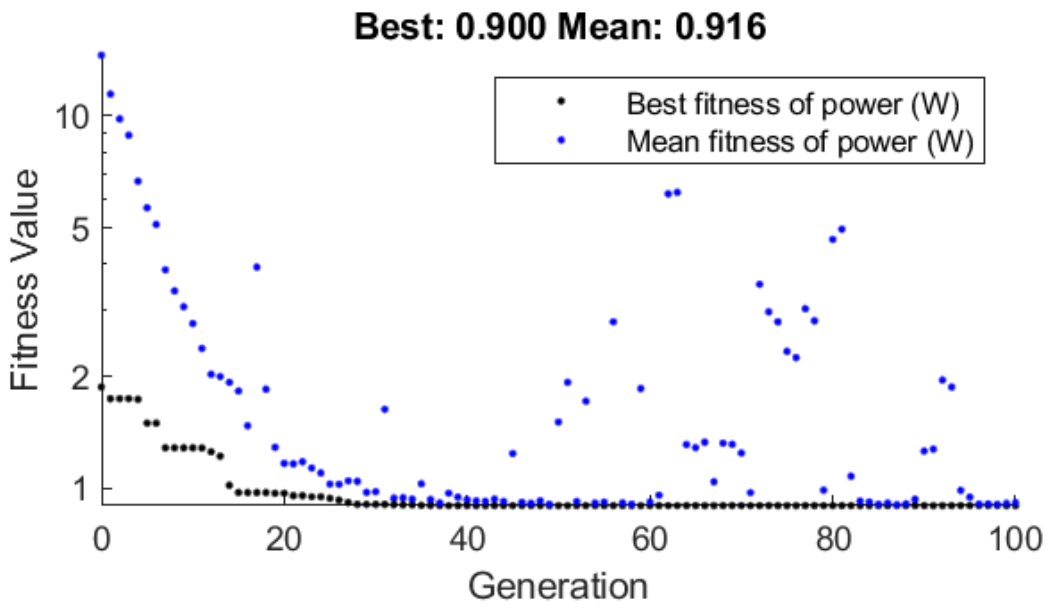

Figure 4.2 100 Mbps Power Fitness Value (W)

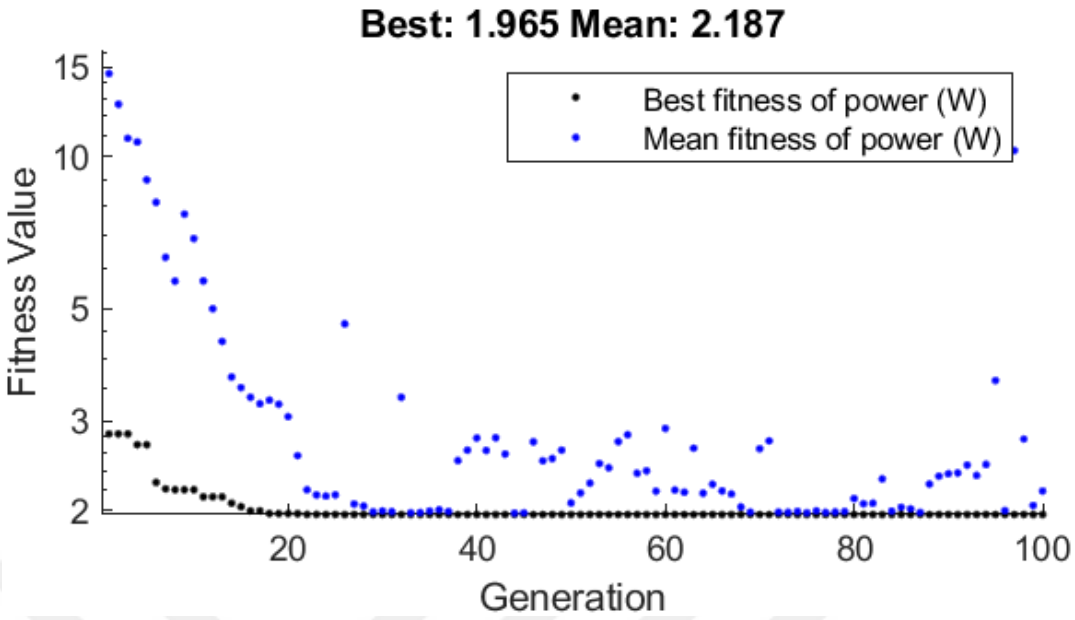

Figure 4.3 200 Mbps Power Fitness Value (W)

Figure 4.4 shows the bandwidth and EA values for PC and SILA in comparison.

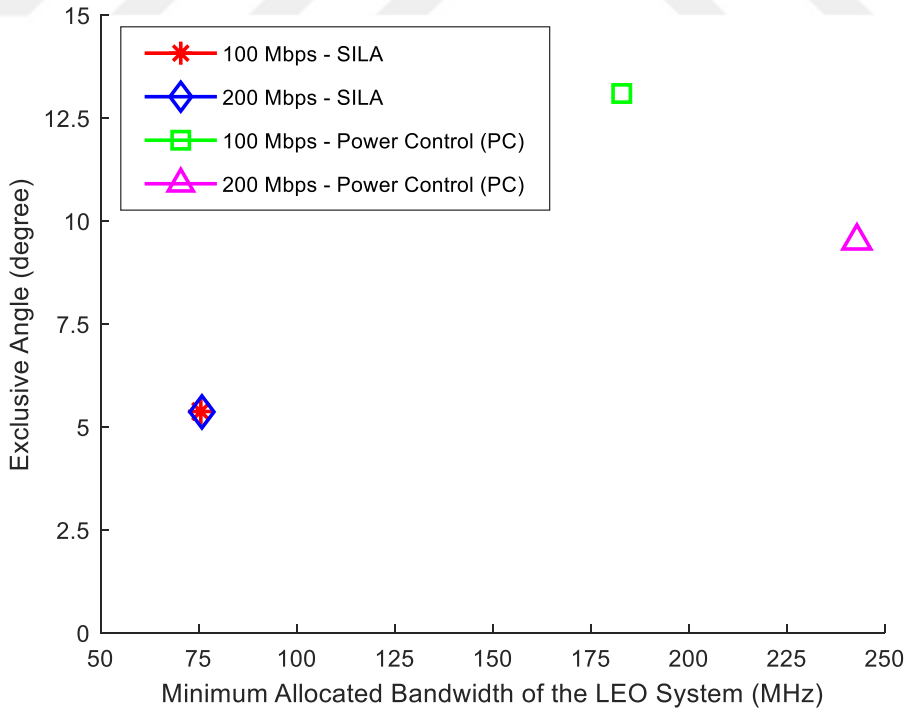

Figure 4.4 Ranges for EA and Bandwidth Allocation in SILA and PC Techniques

Optimal bandwidth and EA results of PC technique can be directly compared to values, which are acquired by the SILA approach [12] in this assessment procedure. Table 4.4 compares the effectiveness of the two methods for reducing interference.

Table 4.4 Performance Assessment of Comparative Results

	PC Technique		SILA Technique		Comparison	
Bit rate (Mbps)	Allocated BW (MHz)	Calculated EA (degree)	Minimum Allocated BW (MHz)	Calculated EA (degree)	Reduction in the BW	Reduction in the EA
100 Mbps	182.93	13.10	75.57	5.38	58.7%	59.0%
200 Mbps	242.91	9.52	75.85	5.37	68.8%	43.6%

Comparative study takes into consideration just Case-1 in [12], which does not use spread spectrum (SS), since current PC approaches do not employ it. Higher bandwidth and EA allocation are clearly needed for the PC approach than for the SILA method. The output power of the SILA method has been set at 10 watts. However, even though the PC approach may lower the optimal power to 0.9 W, the bandwidth demand rises significantly. However, when compared to the EA values produced using the SILA approach [12], the EA results are also too high in PC technique. EZ is often not prioritized in PC methods, however the obtained results indicate that a higher EZ zone should be defined if the EZ approach is selected for PC. Because the PC approach does not consider other link properties as an objective function, it is assumed that a significant increase in the system efficiency cannot be obtained. Comparing SOP findings to MOP results, the effectiveness of SOP findings is also debatable. The MOP methodology prioritizes a number of distinct objectives concurrently, resulting in exceptional system efficiency. Due to the simultaneous assessment of several objective functions, the MOP formulation provides more efficient and suitable solutions. Then, the operator or decision-maker may be able to adjust operational settings (such as bandwidth, EA allocation, and optimum MODCOD) more easily.

4.3. Evaluation of the PC's Contribution to the SILA Technique

The contribution of the power control to the SILA approach is examined in detail in this part. Instead of giving a constant power value to the system, the target is to employ a changeable power value in this analysis. Then, using a MOGA, an optimization problem is developed. In addition, a comparison is made between the final optimization values and the SILA technique's generated values. According to [12], both MODCOD selection-based (Case 1) and MODCOD selection and SS coupled (Case 2) approaches may solve the optimization problem based on the methodology. Taking into account the PC factor, the optimization problem, which is given in equation (3.1) is reformulated.

$EPFD_{S_{GEO_{th}}}$ thresholds, maximum allowed bandwidth for the LEO communication link $B_{LEO_{max}}$, minimum $C/N_{LEO_{th}}$ needs, and $EIRPD_{LEO_{max}}$ limitations for the LEO network are established as the constraints. For a one-to-one comparison with SILA [12], it is important to note that four of the constraints maintained as used in SILA. Table 4.5 lists the MOP's key critical elements.

Table 4.5 MOP Formulation Specifications

Functions	***Constraints***	***Bounds*** ***Case-1*** ***(Case-2)***	***Notes***
$min\,\theta$	$EPFD_{S_{GEO}} \leq EPFD_{S_{GEO_{th}}}$	$\mathrm{DVB-S2X}$	*Acc. to ITU, the GEO earth station's maximum EPFD acceptability limitation is* $-160\ dB(W/m^2)$ *for the 60 cm satellite dish.*
$min\,B_{LEO}$	$B_{LEO} \leq B_{LEO_{max}}$	$0 \leq\ \varphi \leq 20$	*The LEO transmit power variation is 3 dB.*
	$C/N_{LEO} \geq C/N_{LEO_{th}}$	$(1 \leq SF \leq 8)$	*The* $C/N_{LEO_{th}}$ *ratio is employed based on ETSI simulations of DVB-S2X.*
	$EIRPD_{LEO} \leq EIRPD_{LEO_{max}}$	$7.079 \leq P_{T_{LEO}} \leq 14.125$	*The* $EIRPD_{LEO_{max}}$ *value of the LEO system in Ku-Band is* $-13.4\ dBW/4\ KHz$.

In the optimization problem, the EA and the communication link bandwidth are specified as objective functions. Accordingly, the effect of $P_{T_{LEO}}$ on the system's performance is studied in the range of 3 dB. In other words, the impact of the PC functionality on the optimization is examined. The aim is to get the best possible bandwidth and power consumption, as well as the smallest possible assignment of EZ, by choosing the best MODCOD. According to Table 3.3, characteristics of both the LEO and GEO satellite networks are employed to solve the optimization problem. For the sake of comparison, the MOGA optimization settings listed in Table 3.2 have been used.

The optimal values for the PC method's contribution to the SILA approach are computed. For 100 Mbps and 200 Mbps transmission bit rate usage, we calculate the Case-1 and Case-2 results. Figure 4.5-Figure *4.8* presents a comparison Pareto front showing the optimum values for the SILA with PC versus the SILA alone.

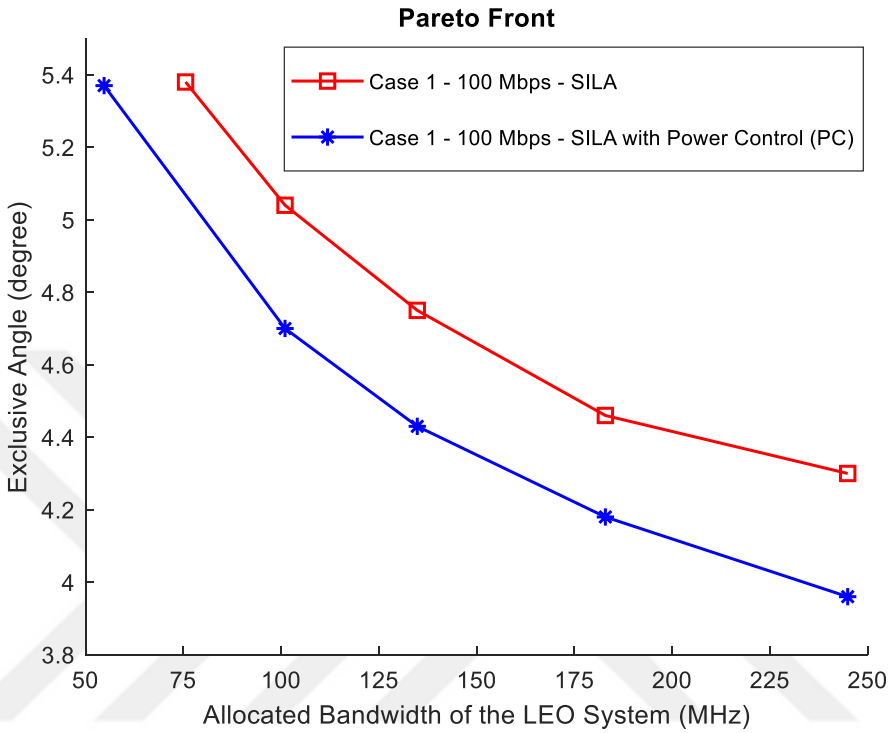

Figure 4.5 Pareto Front Comparison for 100 Mbps, Case-1

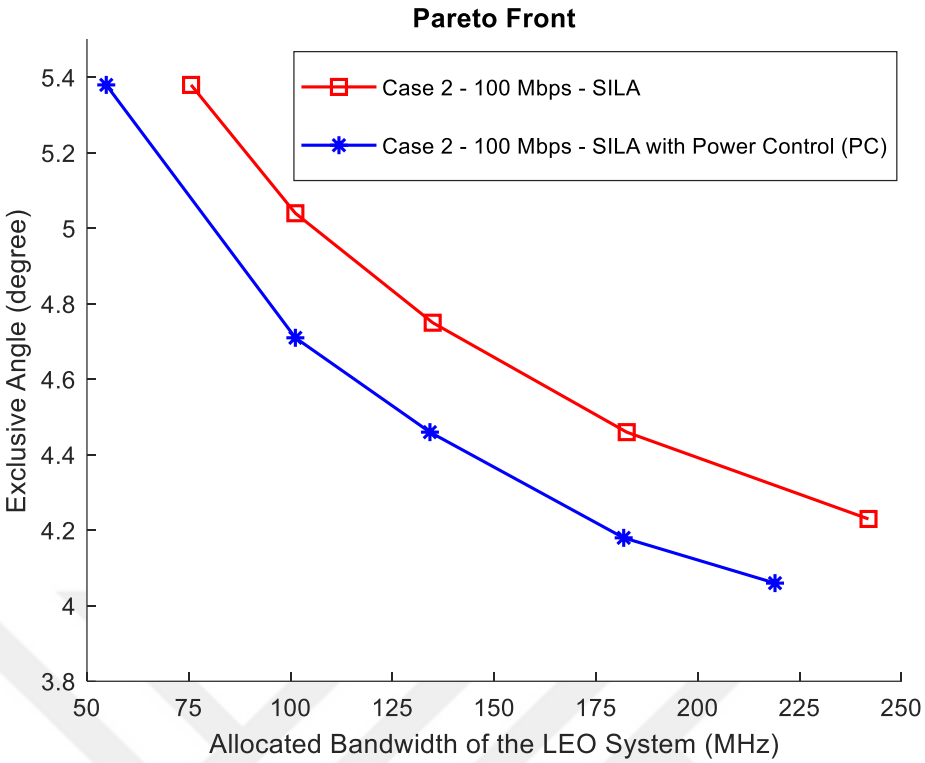

Figure 4.6 Pareto Front Comparison for 100 Mbps, Case-2

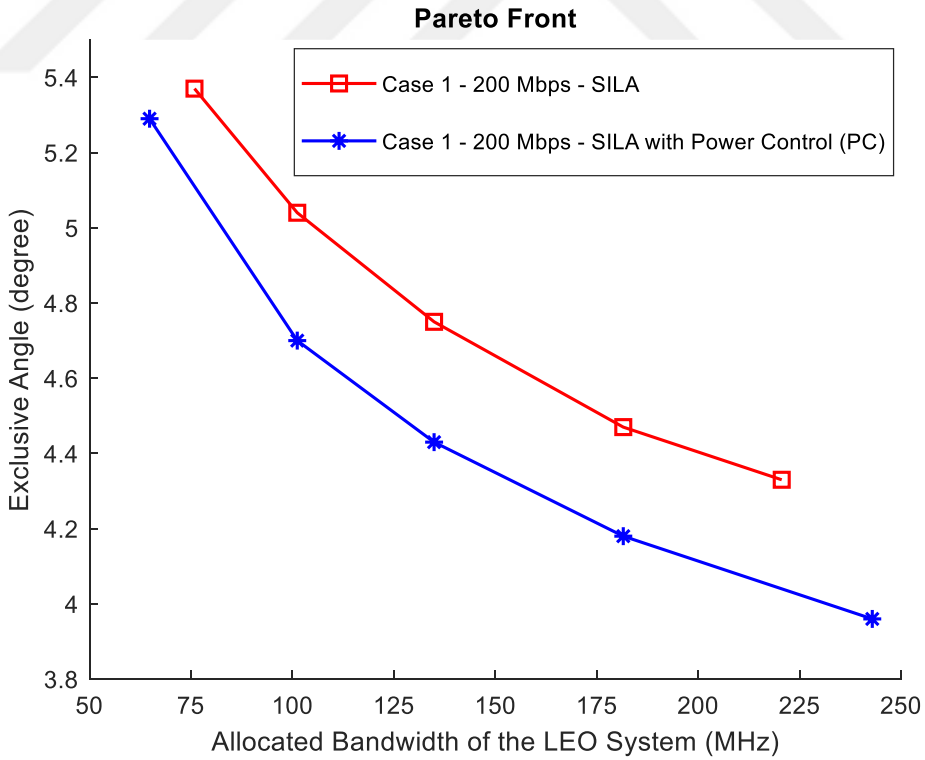

Figure 4.7 Pareto Front Comparison for 200 Mbps, Case-1

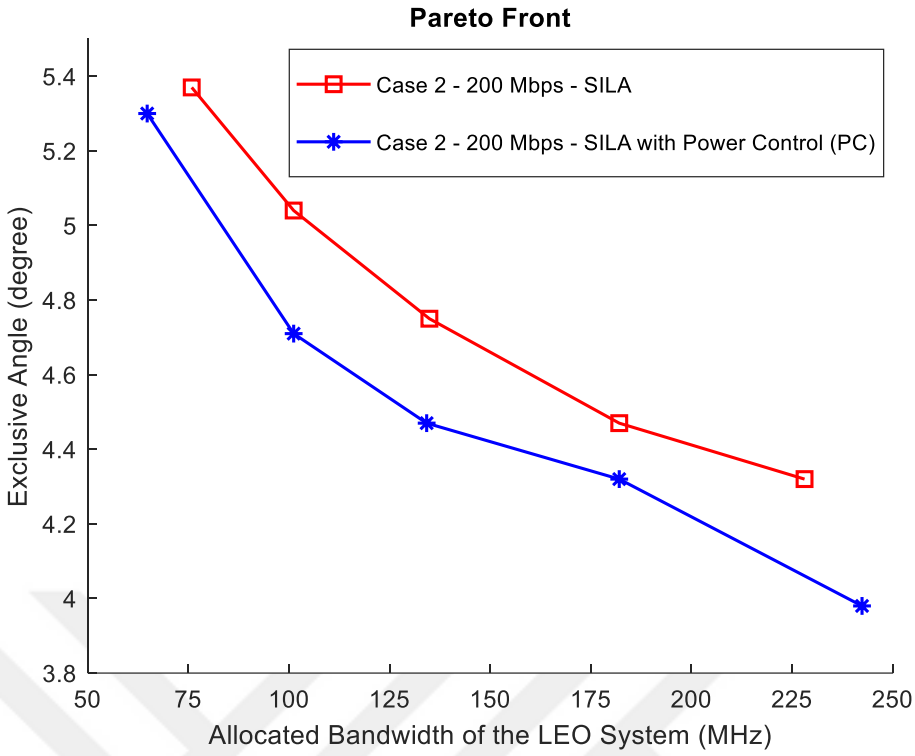

Figure 4.8 Pareto Front Comparison for 200 Mbps, Case-2

Hata! Başvuru kaynağı bulunamadı. shows the EA results for SILA with and without PC contribution.

Table 4.6 Comparison of Minimum EA

Bit Rate (Mbps)	Case	Minimum EA for SILA Technique [12]	Minimum Calculated EA with PC Contribution	Reduction based on a combined approach
100	Case-1	4.30	3.96	8.0%
100	Case-2	4.23	4.06	4.0%
200	Case-1	4.33	3.96	8.5%
200	Case-2	4.32	3.98	8.0%

When the PC method is combined with the SILA technique, EA can be reduced by an additional 8.0% in Case-1 and 4.0% in Case-2, respectively, for 100 Mbps. For 200

Mbps data rate, an enhancement of 8.5% and 8.0%, respectively, can be reached for Case-1 and Case-2. Case-2 may also benefit from SS's ability to allow more flexibility in the setting of operation conditions. Findings shows that when a PC is incorporated to the SILA, the system's efficiency may be improved even further.

CHAPTER 5

EVALUATION AND DISCUSSION

In this chapter, analysis and classification of NGEO-GEO interference mitigation studies in the literature are performed. In addition, contributions of these studies to the co-existing problem solution are examined. The importance of interference mitigation methods and their performance limits are discussed.

It is evident that interference mitigation strategies need to be handled more proactively as the number of NGEO satellites in orbit grows rapidly. Rather than relying on established methodologies, it is critical to build more dynamic mitigation plans via an assessment of the capabilities of next-generation satellites. Figure 5.1 shows the performance assessment of the SILA, PC, and SI techniques under the similar interference conditions.

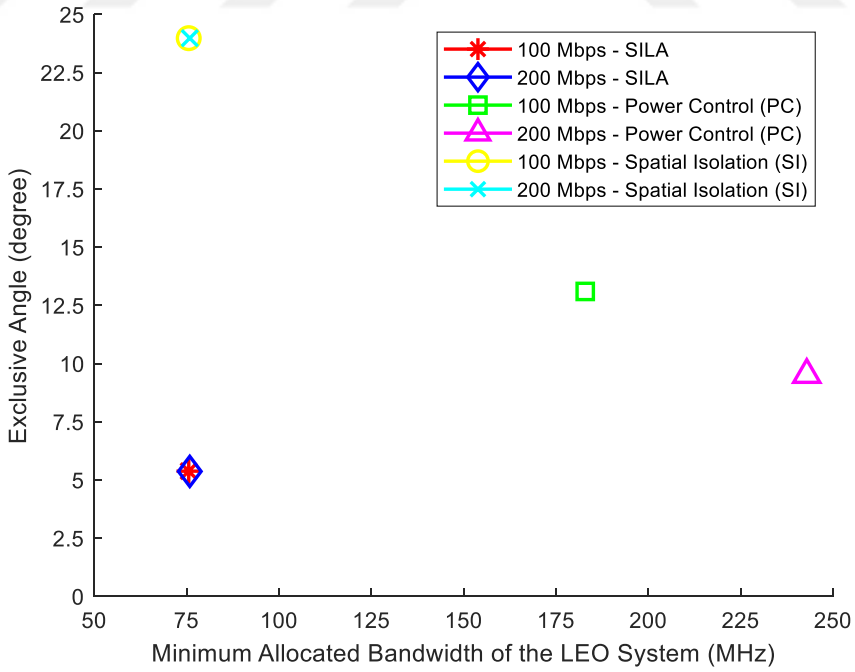

Figure 5.1 Performans Analysis of SILA, PC and SI Techniques

Using a combination of interference mitigation strategies is one of the most effective options. EZ and link adaption techniques are evaluated combined in the SILA [12] as an example of a flexible mitigation solution under varying operating scenarios. It is shown in Section 4.3 that the PC and SILA technique effectively reduce the possibility of co-existent interference. It is also generally known that methods like as beam or satellite drifting, beam hopping, spectrum sharing, spectrum sensing, antenna optimization, NOMA, DL might be useful in mitigating interference. This section also provides a qualitative assessment of these strategies to assist users in determining their suitability. Table 5.1 provides a high-level assessment of the mitigating strategies.

Table 5.1 Assessment of Interference Mitigation Techniques

Interference Mitigation Technique	**Short Description/Features**
Power Control (PC)	Optimizes the power level of the interferer system in order to minimize interference caused by coexistence of NGEO and GEO systems.
Spatial Isolation (SI)	EA and EZ areas are proposed to manage the intensity of interference between various orbital satellites.
Spatial Isolation-Based Link Adaptation (SILA)	Optimizes EZ and communication link operating parameters simultaneously to ensure coexistence operations
Beam or Satellite Drifting	Tilts the directivity of LEO satellites, a technique known as "progressive pitch approach" or turn off specific LEO satellite spot beams to mitigate interference.
Beam Hopping	Properly distributes NGEO traffic demand for coexisting NGEO and GEO systems
Spectrum Sharing	Manages spectrum resources and provides cooperative service approaches for co-existent networks
Spectrum Sensing	Conducts spectrum network analysis and determines the state of spectrum occupancy on various satellite networks
Antenna Optimization	Optimizes antenna gain to minimize or eliminate interference, and provides various specialized antenna options, such as phased arrays, for the interference mitigation
Non-Orthogonal Multiple Access (NOMA)	Establishes a NOMA framework for resolving the interference coordination problem using multi-layer satellite networks (MLSNs)
Deep Learning (DL)	Spectrum sharing via the use of deep learning-based prediction approaches

Table 5.1 shows how these techniques help for the interference coordination. Co-existing interference is critical for satellite networks, as seen by the variety of mitigation solutions presented here. The deployment of mitigation techniques in co-existing interference necessitates further practical ideas. When operators examine PC, beam or satellite drifting, beam hopping, and SILA approaches in Table 5.1, they should prioritize operating conditions first. A more extensive engineering study should be undertaken for the decision-makers or the satellite operators in satellite planning or operating settings, for co-existing NGEO and GEO satellite systems, once any mitigation strategy is established conceptually.

In the application of interference mitigation strategies, the power limitations of various orbital satellites are critical [4,6,8,12]. The gateway or end-user terminals may be improved by taking use of the latest hardware and communication standards (DVB-S2X, SS, ACM, phased array antennas, advanced modems). For instance, the properties of earth stations used in power and power spectral density optimization approaches like as PC and SILA may be well-defined. Selecting an interference mitigation approach should also take into account the earth station's geographic location, such as the equatorial or high/low latitude locations [4,6,13]. System efficiency may be improved by simultaneously prioritizing various functions, which may encourage the user to apply multi-objective methods [12,17,28]. Co-existing interference mitigation problems may be addressed using deep learning (DL) or machine learning (ML) approaches, as shown in [35].

In summary, each of the suggested interference mitigation strategies may have a range of uses depending on the satellite operator's prioritizing of operational and infrastructure needs. Innovative approaches to interference mitigation, such as inter-satellite links or phased array antennas, may offer new possibilities. Nevertheless, with the design of satellite networks with varying capabilities in orbit, it is certain that there will be various research topics devoted to resolving increasingly complicated interference challenges.

CHAPTER 6

CONCLUSION

In this study, the coexistence of LEO and GEO satellite networks has been described and analyzed. A suitable cognitive satellite network model has been developed, and a novel method is proposed to increase the coexistence of these two networks across the equator region by using a typical LEO constellation and a reference GEO satellite system. Based on ITU Equivalent Power Flux Density (EPFD) limitations, a downlink interference formulation from the LEO to the GEO systems has been presented using an exclusion zone (EZ) geometry. In this context, the antenna radiation patterns are crucial in determining the EZ in this scenario. Curve fitting has been used to generate compact radiation patterns from related regulations.

In addition, methods for determining the operating mode of the LEO link for the cognitive network have been presented. System restrictions, resource limits, service needs and communication link requirements have been used to define and solve the multi-objective optimization problem (MOP) based on the genetic algorithm (GA). Pareto frontiers-based solutions to MOPs benefit significantly from the GA technique. An excellent example of addressing MOPs using GA is shown in this study, taking into consideration the selection of the best solutions by taking preferences into account.

Two cases have been investigated in the optimization problem solution in order to obtain the LEO link power spectral density, namely Modulation and Coding (MODCOD) with and without spread spectrum (SS) approaches (Case-1, Case-2). For the first time in co-existence interference mitigation, a combination of MODCOD selection and SS approaches for power spectral density optimization is proposed. Particularly in the second scenario, the spreading factor encourages the usage of greater MODCODs based on the pareto front of the MOP formulation. The Pareto front appears to be a highly efficient method for decision makers or operators because

it allows for a trade-off between exclusive angle (EA) and optimal LEO link operational modes, while also enforcing interference constraints and resource constraints based on the performance limits for both optimization cases. The Spatial Isolation-Based Link Adaptation (SILA) method is the name given to the approach suggested in the thesis.

At data rates of 100 Mbps and 200 Mbps, the optimization results indicate that the EA can be lowered by up to 21.3% and 19.6%, respectively, from the initial anchor point. We found that multi-objective optimization may assist minimize interference among the system and effectively manage LEO link resources in the coexistence of GEO and LEO satellite systems. The optimization results also help to the improvement of LEO satellite communication area without interfering with GEO communication link. This technique presents an ideal solution for coexistence of the GEO and LEO satellite systems that not only eliminates the interference problem but also maintains the link quality of the LEO communication system. The promising findings reported in this thesis may provide valuable information for members of the community, including researchers, decision makers, and/or operators, who are interested in co-existing satellite networks.

The thesis proposes an optimization problem that was solved once with a specific resolution. Then, the optimal solution set was found. Since the conditions and bounds of the optimization algorithm were established with an inclusive approach, the obtained results are applicable to a wide variety of practical scenarios. Acquired typical results can be effectively applied as long as the problem conditions do not completely change. In the event of significant changes to the system conditions, such as the selection of a different LEO system for the interference assessment, it is recommended to rerun the optimization algorithm using the new LEO system parameters. Because of the compact nature of the optimization problem, it will be simple to solve it under new problem conditions. From this perspective, it can be stated that the proposed method is advantageous in terms of practical application.

With the SILA technique presented in the thesis, the selection of optimal operational parameters is proposed. From a practical point of view, the optimal MODCOD choices proposed to the decision maker correspond to proper EZ assignments. Changing the

MODCOD during satellite operation will ensure that the system works at maximum performance. However, both gateway-user terminals should support adaptive coding and modulation (ACM) in this scenario. Although the use of ACM in new generation modems has become widespread, there may be disadvantages such as the additional cost that may arise due to the supply of appropriate equipment and the complexity of the ground station operations.

In this thesis, interference mitigation approaches for co-existing NGEO and GEO systems have been also analyzed, classified, and compared. For the sake of evaluating the methods' performance, both quantitative and qualitative comparisons have been presented. Spatial Isoliation (SI), Power Control (PC), and SILA have been chosen for quantitative assessment because they take into account communication link parameters and spatial limits for the minimization of interference problem. The three methodologies' adaptability to the same interference model is also critical for choosing.

The SI and SILA techniques have been compared using an EA analysis based on the highest modcodes that could be achieved using the SI approach and SILA techniques (Method-1) and the lowest EA values that could be acquired using the MODCOD selection via link optimization (Method-2) in SILA methodology. When the data are analyzed, the SILA approach may be used to minimize the EA for the same MODCOD selection. The EA may also be lowered at a greater rate using the SILA approach in conjunction with MODCOD optimization.

When comparing SILA and PC approaches, the optimization problem of the PC technique has been formulated, and the optimum power, bandwidth, and EA values have been determined initially. Then, the obtained results were compared to those of the SILA method. The PC approach uses more bandwidth and EA than the SILA methodology, according to our research. The MOP formulation in the SILA method has been shown to be superior than the Single-Objective Optimization Problem (SOP) formulation in the PC technique.

Additionally, the PC method's contribution to the SILA technique was thoroughly investigated. When the PC approach is used in conjunction with the SILA technique, it has been shown that system efficiency may be boosted by up to 8.0% and 8.5% for

100 Mbps and 200 Mbps data rate uses, respectively. Using a variety of interference mitigation techniques together has been found to improve system performance.

Moreover, other researches in the literature have been examined and contributions have been described in depth for qualitative comparison. The pertinent research goals have been summarized, and a qualitative comparison with the thesis study is given. An additional categorization of interference mitigation approaches has also been performed. Finally, recommendations and overall assessments of these findings have been presented.

Different algorithms may be used to address the MOP issue. The use of artificial intelligence methods (machine learning and/or deep learning) instead of standard optimization algorithms may enable link adaptability and optimum satellite positioning here. Particularly, phased array antennas, inter-satellite connectivity, and machine learning/deep learning (ML/DL) methods are mentioned as creative ideas that may help solve present and future interference concerns. With the increasing complexity of next-generation satellite networks, the interference mitigation strategies discussed here may need to be enhanced further.

On the other hand, tens of thousands of satellites in low-Earth orbit seem to be operational in the coming years. Besides the interference problem, satellite collisions or space debris in low-Earth orbit should be taken into consideration. As the LEO satellites are likely to be used more widely for Internet of Things (IoT) devices, security is an important issue. Consequently, in the upcoming years, substantial research into precautions or even countermeasures for safer LEO/GEO satellite networks is also expected.

REFERENCES

[1] Y. Su, Y. Liu, Y. Zhou, J. Yuan, H. Cao, J. Shi, "Broadband LEO Satellite Communications: Architectures and Key Technologies," *IEEE Wireless Commun*, vol. 26, pp. 55-61, 2019.

[2] I. Portillo, BG. Cameron, EF. Crawley, "A Technical Comparison of Three Low Earth Orbit Satellite Constellation Systems to Provide Global Broadband," *Acta Astronautica*, vol. 159, pp. 123-135, 2019.

[3] C. Park, C. Kang, Y. Choi, C. Oh, "Interference Analysis of Geostationary Satellite Networks in the Presence of Moving Non-Geostationary Satellites," in *2nd International Conference on Information Technology Convergence and Services (ITCS)*, Cebu, Philippines, 2010.

[4] J. LI, M. LI, W. LI, "Satellite communication on the non-geostationary system and the geostationary system in the Fixed-satellite service," in *28th Wireless and Optical Communications Conference (WOCC)*, Beijing, China, 2019.

[5] RC. Santiago, VY. Kontorovitch, ML. Barrón, "Modified methodology for computing interference in LEO satellite environments," *Int J Satell Commun Netw.*, vol. 21, pp. 547-560, 2003.

[6] ICM Nobre, JM. Fortes, "On the protection of fixed service receivers from the interference generated by non-GSO satellite systems operating in the 3.7-4.2 GHz band," *Int J Satell Commun Netw.*, vol. 36, pp. 383-401, 2018.

[7] SK. Sharma, S. Chatzinotas, B. Ottersten, "In-line Interference Mitigation Techniques for Spectral Coexistence of GEO and NGEO satellites," *Int J Satell Commun Netw.*, vol. 34, pp. 11-39, 2016.

[8] H. Wang, C. Wang, J. Yuan, Y. Zhao, R. Ding, W. Wang, "Coexistence Downlink Interference Analysis Between LEO System and GEO System in Ka Band," in *IEEE/CIC International Conference on Communications in China (ICCC)*, Beijing, China, 2018.

[9] "Simulation methodologies for determining statistics of short-term interference between co-frequency, codirectional non-geostationary-satellite orbit fixed-satellite service systems in circular orbits and other non-geostationary fixed

satellite service systems incircular orbits or geostationary-satellite orbit fixed-satellite service networks," ITU-R S.1325-3, 2003.

[10] "Interference Mitigation Techniques to Facilitate Coordination between Non-Geostationary-Satellite Orbit Mobile-Satellite Service Feeder Links and Geostationary-Satellite Orbit Fixed-Satellite Service Networks in the Bands 19.3-19.7 GHz and 29.1-29.5 GHz," ITU-R S.1419, 1999.

[11] H. Zhang, "Spatial Isolation Methodology Analysis in Ka Band for LEO-GEO Coexistence Systems," in *International Conference on Robots & Intelligent System (ICRIS)*, Changsha, China, 2018.

[12] F. Öztürk, A. Kara, "Exclusion Zone Minimization and Optimal Operational Mode Selection for Co-Existent Geostationary and Non-Geostationary Satellites," *Int J Satell Commun Netw.*, vol. 40, pp. 191-203, 2021.

[13] T. Li, J. Jin, W. Li, Z. Ren, L. Kuang, "Research on interference avoidance effect of OneWeb satellite constellation's progressive pitch strategy," *Int J Satell Commun Netw.*, vol.39, pp. 524-538, 2021.

[14] JMP. Fortes, R. Sampaio-Neto, JEA. Maldonado, "An analytical method for assessing interference in an environment involving NGSO satellite networks," *Int J Satell Commun.*, vol. 17, pp. 399-419, 1999.

[15] SK. Sharma, S. Chatzinotas, B. Ottersten, "Interference alignment for spectral coexistence of heterogeneous networks," *EURASIP J Wireless Commun Netw.*, 46, 2013.

[16] A. Pourmoghadas, SK. Sharma, S. Chatzinotas, B. Ottersten, "Cognitive Interference Management Techniques for the Spectral Co-existence of GSO and NGSO Satellites," in *International Conference on Wireless and Satellite Systems (WISATS)*, Cardiff, UK, 2016.

[17] R. Li, P. Gu, C. Hua, "Optimal Beam Power Control for Co-Existing Multibeam GEO and LEO Satellite System," in *11th International Conference on Wireless Communications and Signal Processing (WCSP)*, Xi'an, China, 2019.

[18] C. Wang, D. Bian, S. Shi, J. Xu, G. Zhang, "A Novel Cognitive Satellite Network With GEO and LEO Broadband Systems in the Downlink Case," *IEEE Access*, vol. 6, pp. 25987-26000, 2018.

[19] SK. Sharma, S. Chatzinotas, B. Ottersten, "Cognitive beamhopping for spectral coexistence of multibeam satellites," *Int J Satell Commun Netw.*, vol. 33, pp. 69-91, 2015.

[20] C. Yang, Q. Zhang, Q Tian, X. Xin, B. Liu, L. Zhang, Y. Shen, Y. Tao, D. Chen, N. Xin, "In-line interference mitigation method based on Adaptive modulation and coding for satellite system," in *16th International Conference on Optical Communications and Networks (ICOCN)*, Wuzhen, China, 2017.

[21] C. Zhang, J. Jin, H. Zhang, T. Li, "Spectral Coexistence between LEO and GEO Satellites by Optimizing Direction Normal of Phased Array Antennas," *China Commun.*, vol. 15, pp. 18-27, 2018.

[22] A. Pourmoghadas, SK. Sharma, S. Chatzinotas, B. Ottersten, "On the spectral coexistence of GSO and NGSO FSS systems: PC mechanisms and a methodology for inter-site distance determination," *Int J Satell Commun Netw.*, vol. 35, pp. 443-459, 2017.

[23] F. Vatalaro, GE. Corazza, C. Caini, C. Ferrarelli, "Analysis of LEO, MEO, and GEO global mobile satellite systems in the presence of interference and fading," *IEEE J Sel A. Commun.*, vol. 13, pp. 291-300, 2006.

[24] J. Tong, C. Wang, X. Zhao, G. Cui, W. Wang, "Cooperative Beam Association and Power Allocation in UD-LEO Satellite Communication Networks: A Spectrum Sharing Manner," *Electronics*, vol. 11, pp. 299, 2022.

[25] J. Tang, D. Bian, G. Li, J. Hu, J. Cheng, "Resource Allocation for LEO Beam-Hopping Satellites in a Spectrum Sharing Scenario," *IEEE Access*, vol. 9, pp. 56468-56478, 2021.

[26] P. Gu, R. Li, C. Hua, R. Tafazolli, "Cooperative Spectrum Sharing in a Co-existing LEO-GEO Satellite System," in *GLOBECOM IEEE Global Communications Conference*, Taipei, Taiwan, 2020.

[27] P. Gu, R. Li, C. Hua, R. Tafazolli, "Dynamic Cooperative Spectrum Sharing in a Multi-Beam LEO-GEO Co-Existing Satellite System," *IEEE Transactions on Wireless Communications*, vol. 21, pp. 1170-1182, 2022.

[28] M. Jia, Z. Li, X. Gu, Q. Guo, "Joint Multi-beam Power Control for LEO and GEO Spectrum-sharing Networks," in *IEEE/CIC International Conference on Communications in China (ICCC)*, Xiamen, China, 2021.

[29] Y. Wang, X. Ding, G. Zhang, “A Novel Dynamic Spectrum-Sharing Method for GEO and LEO Satellite Networks,” *IEEE Access*, vol. 8, pp. 147895-147906, 2020.

[30] H. Wang, R. Ren, D. Qu, G. Zhang, “A Radio Environment Mapping Based Spectrum Awareness for Cognitive Space Information Network with GEO and LEO Coexistence,” in *International Conference on Wireless Communications and Signal Processing (WCSP)*, Wuhan Hubei, China, 2020.

[31] C. Zhang, C. Jiang, J. Jin, S. Wu, L. Kuang, S. Guo, “Spectrum Sensing and Recognition in Satellite Systems,” *IEEE Transactions on Vehicular Technology*, vol. 68, pp. 2502-2516, 2019.

[32] R. Ge, D. Bian, J. Cheng, K. An, J. Hu, G. Li, “Joint User Pairing and Power Allocation for NOMA-Based GEO and LEO Satellite Network,” *IEEE Access*, vol. 9, pp. 93255-93266, 2021.

[33] R. Ge, D. Bian, K. An, J. Cheng, H. Zhu, “Performance Analysis of Cooperative Nonorthogonal Multiple Access Scheme in Two-Layer GEO/LEO Satellite Network,” *IEEE Systems Journal*, vol. 16, pp. 1-11, 2021.

[34] C. Wang, D. Bian, G. Zhang, J. Cheng, Y. Li, “A Novel Dynamic Spectrum-Sharing Method for Integrated Wireless Multimedia Sensors and Cognitive Satellite Networks,” *Sensors*, vol. 18, pp. 3904, 2018.

[35] X. Ding, L. Feng, Y. Zou, G. Zhang, “Deep Learning Aided Spectrum Prediction for Satellite Communication Systems,” *IEEE Transactions on Vehicular Technology*, vol. 69, pp. 16314-16319, 2020.

[36] “Second generation framing structure, channel coding and modulation systems for Broadcasting, Interactive Services, News Gathering and other broadband satellite applications; Part 2: DVB-S2 Extensions,” ETSI EN 302 307-2, V1.2.1, Digital Video Broadcasting (DVB), 2020.

[37] N. Mazzali, S. Boumard, J. Kinnunen, BS. MR, M. Kiviranta, N. Alagha, “Enhancing mobile services with DVB-S2X superframing,” *Int J Satell Commun Netw.*, vol. 36, pp. 503-527, 2018.

[38] “DVB-S2 Adaptive Coding and Modulation for Broadband Hybrid Satellite Dialup Applications,” ETSI TS 102 441, V1.1.1, Digital Video Broadcasting (DVB), 2005.

[39] “Second Generation DVB Interactive Satellite System (DVB-RCS2); Part 1: Overview and System Level specification,” ETSI TS 101 545-1, V1.3.1, Digital Video Broadcasting (DVB), 2020.

[40] C. Popper, M. Strasser, S. Capkun, “Anti-jamming broadcast communication using uncoordinated spread spectrum techniques,” *IEEE J Sel A Commun.,* vol. 28, pp. 703-715, 2010.

[41] Kohl M, Jondral F., “Interference on satcom up-links and its suppression,” *Int J Satell Commun.,* vol. 16, pp. 147-153, 1998.

[42] RDJ. van Nee, HS. Misser, R. Prasad, “Direct-sequence spread spectrum in a shadowed Rician fading and land-mobile satellite channel,” *IEEE J Sel A Commun*., vol. 10, pp. 350-357, 1992.

[43] K. Cheun, K. Choi, H. Lim, K. Lee, “Antijamming performance of a multicarrier direct-sequence spread-spectrum system,” *IEEE Trans Commun,* vol. 47, pp. 1781-1784, 1999.

[44] P. Kim, A. Vanelli-Coralli, M. Villanti, R. Pedone, S. Cioni, M. Neri, C. Palestini, M. Papaleo, H. Lee, GE. Corazza, “Direct sequence spectrum spreading techniques for next generation mobile broadband satellite services,” *Int J Satell Commun Netw.*, vol. 28, pp. 157-181, 2010.

[45] A. Jamalipour, A. Ogawa, “Packet admission control in a direct-sequence spread-spectrum LEO satellite communications network,” *IEEE J Sel A Commun*., vol. 15, pp. 1649-1656, 1997.

[46] G. Chiandussi, M. Codegone, S. Ferrero, FE. Varesio, “Comparison of multi-objective optimization methodologies for engineering applications,” *Comput. Math. Appl*., vol. 63, pp. 912–942, 2012.

[47] DE. Şala, Y. Dalveren, A. Kara, M. Derawi, “Design and Optimization of Piezoelectric-Powered Portable UV-LED Water Disinfection System,” *Appl. Sci.*, vol. 11, pp. 3007, 2021.

[48] AI. Aravanis, BS. MR, P. Arapoglou, G. Danoy, PG. Cottis, B. Ottersten, “Power Allocation in Multibeam Satellite Systems: A Two-Stage Multi-Objective Optimization,” *IEEE Trans on Wireless Commun.,* vol. 14, pp. 3171-3182, 2015.

[49] JC. Ferreira, CM. Fonseca, A. Gaspar-Cunha, "Methodology to select solutions from the pareto-optimal set: a comparative study," in *Proceedings of the 9th annual conference on Genetic and evolutionary computation (GECCO '07)*, London, England, 2007.

[50] Q. Long, C. Wu, T. Huang, X. Wang, "A genetic algorithm for unconstrained multi-objective optimization," *Swarm and Evolutionary Computation*, vol. 22, pp. 1-14, 2015.

[51] VS. Summanwar, VK. Jayaraman, BD. Kulkarni, HS. Kusumakar, K. Gupta, J. Rajesh, "Solution of constrained optimization problems by multi-objective genetic algorithm," *Computers & Chemical Engineering*, vol. 26, pp. 1481-1492, 2002.

[52] JFA. Madeira, H. Rodrigues, H. Pina, "Multi-objective optimization of structures topology by genetic algorithms," *Advances in Engineering Software*, vol. 36, pp. 21-28, 2005.

[53] H. Link, D. Weuster-Botz, "Genetic algorithm for multi-objective experimental optimization," *Bioprocess Biosyst Eng*, 29, pp. 385–390, 2006.

[54] "Satellite antenna radiation patterns for non-geostationary orbit satellite antennas operating in the fixed-satellite service below 30 GHz," ITU-R S.1528, 2001.

[55] "Reference FSS earth-station radiation patterns for use in interference assessment involving non-GSO satellites in frequency bands between 10.7 GHz and 30 GHz," ITU-R S.1428, 2001.

[56] "Radio Regulations," ITU-R, Article 22; pp. 279-298, 2016.

[57] "Application for Fixed Satellite Service," WorldVu Satellites Limited, SAT-LOI-20160428-00041. 2017, Accessed: Nov. 23, 2020. [Online]. Available: https://fcc.report/IBFS/SAT-LOI-20160428-00041

[58] MA. Diaz, N. Courville, C. Mosquera, G. Liva, GE. Corazza, "Non-Linear Interference Mitigation for Broadband Multimedia Satellite Systems," in *International Workshop on Satellite and Space Communications*, 2007.

[59] CA Balanis, *Antenna Theory Analysis and Design*, Wiley: Hoboken, NJ 07030, 2005, pp. 94-98.

[60] M. Richharia, LD. Westbrook, *Satellite Systems for Personal Applications Concepts And Technology*, Wiley: Chichester, West Sussex PO19 8SQ, UK, 2010, pp. 123-159.

[61] A. Gilat, *MATLAB An Introduction with Applications*, Wiley: Hoboken, NJ, 2017, pp. 261-274.

[62] D. Roddy, *Satellite Communications*, NY, USA: The McGraw-Hill Companies, Inc., 2006, pp. 283-303.

[63] JN. Pelton, S. Madry, S. Camacho-Lara, *Handbook of Satellite Applications*, Springer: Cham, Switzerland, 2017, pp. 464-479.

[64] B. Scheers, VL. Nir, "A Modified Direct-Sequence Spread Spectrum Modulation Scheme For Burst Transmissions," 2010, Accessed on: Feb. 20, 2021, [Online]. Available: https://www.researchgate.net/publication/228705639

[65] MA. Abu-Rgheff, *Introduction to CDMA Wireless Communications*, Academic Press: 84 Theobald's Road, London WC1X 8RR, UK, 2007, pp. 153-194.

[66] "Second Generation DVB Interactive Satellite System (DVB-RCS2); Part 4: Guidelines for Implementation and Use of EN 301 545-2," ETSI TS 101 545-4, V1.1.1, Digital Video Broadcasting (DVB), 2014.

[67] M. Ehrgott, *Multicriteria Optimization*, Springer: Berlin, Germany, 2005, pp. 23-38.

[68] JS. Gero, *Design Optimization*, Academic Press: London NW1 7DX, UK, 1985, pp. 193–227.

[69] CA. Coello Coello, "Theoretical and numerical constraint-handling techniques used with evolutionary algorithms: a survey of the state of the art," *Computer Methods in Applied Mechanics and Engineering*, vol. 191, pp. 1245–1287, 2002.

APPENDICES

A. ITU-R S. 1528 Antenna Pattern Formulation

The reference pattern for a LEO satellite transmit antenna with an antenna aperture diameter to wavelength ratio of $D/\lambda < 35$ is defined by ITU-R S.1528 as follows

$$G(\varphi) = G_m - 3(\varphi/\varphi_b)^2 \qquad for\ \varphi_b < \varphi < Y$$

$$G(\varphi) = G_m + L_s - 25\log(\varphi/Y) \qquad for\ Y < \varphi < Z$$

$$G(\varphi) = L_F \qquad for\ Z < \varphi < 180^{\circ}$$

for $L_s = -6.75; \quad Y = 1.5\varphi_b$

$$G(\varphi) = 20\log(D/\lambda) + 5.65 - 25\log(\varphi/\varphi_b)$$

$$for\ 1.5\varphi_b < \varphi < Z$$

where $Z = Y \times 10^{0.04(G_m + L_s - L_F)}$, $Y = \varphi_b(-L_s/3)^{1/2}$, L_s is the main beam and near-in side-lobe mask cross point (dB) below the peak gain, L_F is the far-out side-lobe level (dBi), φ_b is the one half the 3 dB beamwidth in the plane of interest at the highest off-axis angle, L_s is the main beam and near-in side-lobe mask cross point (dB) below peak gain, D is the diameter of antenna (m) and $G_m = 20\log(D/\lambda)$ represents the maximum gain in the main lobe (dBi). For a LEO satellite $L_s = -6.75$ and $Y = 1.5\varphi_b$, $2\varphi_b$ being the half power beamwidth. The value of L_F is 0 dBi for ideal patterns.

B. ITU-R S. 1428-1 Antenna Pattern Formulation

According to ITU-R S.1428-1, when there are several interfering sources whose locations change significantly over time, the quantity of interference received necessarily relies on the troughs as well as the peaks in the victim's or source's antenna side lobe gain pattern. In this context, ITU-R S.1428 suggests the following reference earth station pattern for both GEO and LEO communication links

for antennas having $20 \leq \frac{D}{\lambda} \leq 25$:

$$G(\theta) = G_{max} - 2.5 \times 10^{-3} \left(\frac{D}{\lambda}\theta\right)^2 \qquad for\ 0 < \theta < \theta_m$$

$$G(\theta) = G_1 \qquad for\ \theta_m \leq \theta < \left(\frac{95\lambda}{D}\right)$$

$$G(\theta) = 29 - 25 \log \theta \qquad for\ 95\frac{\lambda}{D} \leq \theta < 33.1°$$

$$G(\theta) = -9 \qquad for\ 33.1° < \theta \leq 80°$$

$$G(\theta) = -5 \qquad for\ 80° < \theta \leq 180°$$

for $25 \leq \frac{D}{\lambda} \leq 100$:

$$G(\theta) = G_{max} - 2.5 \times 10^{-3} \left(\frac{D}{\lambda}\theta\right)^2 \qquad for\ 0 < \theta < \theta_m$$

$$G(\theta) = G_1 \qquad for\ \theta_m \leq \theta < \left(\frac{95\lambda}{D}\right)$$

$$G(\theta) = 29 - 25 \log \theta \qquad for\ 95\frac{\lambda}{D} \leq \theta \leq 33.1°$$

$$G(\theta) = -9 \qquad for\ 33.1° < \theta \leq 80°$$

$$G(\theta) = -4 \qquad for\ 80° < \theta \leq 120°$$

$$G(\theta) = -9 \qquad for\ 120° < \theta \leq 180°$$

where;

$$G_{max} = 20\log\left(\frac{D}{\lambda}\right) + 7.7\ dBi$$

$$G_1 = 29 - 25\log\left(95\frac{\lambda}{D}\right)$$

$\theta_m = \frac{20\lambda}{D}\sqrt{G_{max} - G_1}$ degrees

for $\frac{D}{\lambda} > 100$:

$$G(\theta) = G_{max} - 2.5 \times 10^{-3}\left(\frac{D}{\lambda}\theta\right)^2 \qquad for\ 0 < \theta < \theta_m$$

$$G(\theta) = G_1 \qquad for\ \theta_m \leq \theta < (\theta_r)$$

$$G(\theta) = 29 - 25\log\theta \qquad for\ \theta_r \leq \theta < 10°$$

$$G(\theta) = 34 - 30\log\theta \qquad for\ 10° \leq \theta < 34.1°$$

$$G(\theta) = -12 \qquad for\ 34.1° \leq \theta < 80°$$

$$G(\theta) = -7 \qquad for\ 80° \leq \theta < 120°$$

$$G(\theta) = -12 \qquad for\ 120° \leq \theta \leq 180°$$

where;

$$G_{max} = 20\log\left(\frac{D}{\lambda}\right) + 8.4\ dBi$$

$$G_1 = -1 + 15\log\left(\frac{D}{\lambda}\right)\ dBi$$

$\theta_m = \frac{20\lambda}{D}\sqrt{G_{max} - G_1}$ degrees

$\theta_r = 15.85\left(\frac{D}{\lambda}\right)^{-0.6}$ degrees